

Forschungszentrum Karlsruhe

Technik und Umwelt

Wissenschaftliche Berichte

FZK 6049

**Comparison of Two Radiative Transfer Codes with Respect to the
Modeling of the Line Mixing Effect**

A. V. Polyakov*, B. Funke, G. Stiller, H. Fischer, E. M. Shulgina*

Institut für Meteorologie und Klimaforschung

***Sankt Petersburg State University
Research Institute of Physics**

**Forschungszentrum Karlsruhe GmbH, Karlsruhe
1997**

Kurzfassung

Vergleich zweier Strahlungsübertragungsalgorithmen hinsichtlich der Modellierung des Line-Mixing-Effektes

Hohe Anforderungen an die Genauigkeit von Strahlungsübertragungs-Rechnungen wurden zuerst durch die Verfügbarkeit von neuen, verfeinerten Spektrometern mit verbesserten radiometrischen Eigenschaften (unter ihnen das MIPAS Spektrometer) erzeugt. Dies führte dazu, daß eine Reihe von speziellen Effekten, wie der Line-Mixing-Einfluß (LM Einfluß), bei der Strahlungsübertragungsrechnung berücksichtigt werden müssen. In der vorliegenden Studie wurden zwei verschiedene Methoden zur Berechnung der atmosphärischen Transmission und Strahldichte unter Berücksichtigung des Line-Mixing-Effektes verwendet und miteinander verglichen. Eine dieser Methoden wurde im IMK entwickelt und wird dort auch angewendet. Sie modelliert die komplexe Relaxationsmatrix über die Anwendung des sog. "Exponential Power Gap Law" wie es von Strow et al. eingeführt wurde. Die andere Methode wird als ABC-Methode (Adjusted Branch Coupling) bezeichnet. Sie war ursprünglich von M.V. Tonkov und N.N. Filippov entwickelt worden und wird an der Staats-Universität St. Petersburg (SPbSU) eingesetzt. Diese neue empirische Methode zur Berechnung der Bandenform unter Berücksichtigung des LM-Effektes baut auf einem Modell der starken Stöße (strong-collision model) mit abgeschwächter Kopplung zwischen den Bandenzweigen auf.

Im ersten Teil der Studie wurden die Berechnungen mit den beiden Methoden mit Labor-Transmissionmessungen verglichen, die im Spektralbereich um 2093 cm^{-1} im Q-Zweig der 14-2 Vibrationsbande von CO_2 aufgenommen wurden, wo ein merklicher LM-Effekt beobachtet wird. Zwei Labor-Absorptionsspektren, die mit hoher spektraler Auflösung und großer Genauigkeit gemessen worden sind, nämlich ein Spektrum von reinem CO_2 und ein Spektrum von CO_2 in N_2 , wurden im Vergleich benutzt. Es zeigte sich, daß beide Methoden eine korrekte qualitative Beschreibung des Line-Mixing-Effektes liefern. Die Abweichungen zwischen den berechneten und experimentellen Transmissionen sind höchstens etwa 0.02 für den IMK-Algorithmus und 0.06 für die SPbSU Methode. Der größere Fehler der SPbSU Methode wird wahrscheinlich durch eine spektrale Verschiebung des Absorptionsmaximums erzeugt, die für diese Methode spezifisch ist, obwohl sie eine korrekte qualitative Beschreibung der Bandenform liefert.

Der zweite Teil der Studie ist einem Vergleich der längs eines atmosphärischen optischen Pfades abgestrahlten Strahldichte gewidmet, die mit Hilfe der beiden Methoden berechnet wurde. Die Transmissionsfunktionen und die atmosphärische Strahldichte wurden im spektralen Intervall $719 - 722\text{ cm}^{-1}$ berechnet, das im kurzwelligen Flügel der $15\text{ }\mu\text{m}$ CO_2 -Bande liegt. Hier ist der Q-Zweig der 5-2 Bande des CO_2 mit einem merklichen LM-Effekt zu finden. Die Berechnungen wurden für Tangentenhöhen zwischen 6 und 35 km ausgeführt, weil dort der maximale LM-Einfluß auf die abgestrahlte Strahldichte erwartet werden kann. Obwohl sich die Studie an der Auswertung von Messungen mit Instrumenten mit endlicher spektraler Auflösung orientiert, wurde der Vergleich für monochromatische Transmissionen und Strahldichten durchgeführt. Dies erlaubte es, die Unterschiede zwischen den beiden Methoden genauer

zu untersuchen. Die Berechnungen der abgestrahlten Strahldichte zeigten qualitative Übereinstimmung der beiden Methoden. Allerdings liefert das SPbSU Modell - die ABC-Methode - einen höheren LM-Effekt im Flügelbereich des Q-Zweigs, und einen kleineren LM-Effekt im Bereich des Q-Zweig-Zentrums, verglichen mit der IMK-Methode, für alle Tangentenhöhen. Bei starker CO₂-Absorption unterscheiden sich die Werte des LM-Effekts der beiden Methoden um einen Faktor 2 im Q-Zweig-Flügel. Die Unterschiede der beiden Methoden in der abgestrahlten Strahldichte erreichen in manchen Fällen etwa 4 mW/(m² sr cm⁻¹).

Abstract

High requirements with regard to the accuracy of radiative transfer calculations caused first by the availability of new refined spectral instruments with enhanced radiometric characteristics (among them the MIPAS spectrometer) resulted in a necessity to take into account correctly various special effects such as the Line Mixing (LM) influence. In the present study, two different methods of computing the atmospheric transmittance and radiance with accounting for the LM effect have been used and compared. One of these methods was developed and is applied at the IMK. It models the complex relaxation matrix by applying the Exponential Power Gap Law as introduced by Strow et al. [1994]. The other method is referred to as the ABC (Adjusted Branch Coupling) method. It was originally developed by M.V. Tonkov and N.N. Filippov and used for atmospheric applications at the SPbSU. This new empirical method of band shape calculation taking into account the LM effect is based on a strong collision model with weakened interbranch coupling.

In the first part of the study, the calculations by the two methods were compared with laboratory transmittance measurements near 2093 cm^{-1} in the Q-branch of the 14-2 vibration band of CO_2 , where a noticeable LM effect is observed. Two laboratory absorption spectra registered with high accuracy and spectral resolution - the spectrum of pure CO_2 and the spectrum of CO_2 in N_2 - were used in the comparison. It turned out that both methods provide a correct qualitative description of the Line Mixing effect. Maximum differences between calculated and experimental transmittances are about 0.02 and 0.06 for the IMK and SPbSU methods. The larger error of the SPbSU method is likely to be caused by an absorption maximum shift specific for the method, though it gives a correct qualitative description of the band shape.

The second part of the study is dedicated to mutual comparison of slant path outgoing radiation calculations by the two methods. The transmittance functions and atmospheric radiation were computed in the $719 - 722\text{ cm}^{-1}$ spectral interval of the short-wave wing of the $15\text{ }\mu\text{m}$ CO_2 . Here, the Q-branch of the 5-2 band of CO_2 with a detectable LM effect is located. The calculations were carried out for tangent heights of 6 - 35 km, where the maximum LM influence on outgoing radiation may be expected. Though the study is oriented to processing the measurements by instruments with finite spectral resolution, the comparison was performed for monochromatic transmittance and radiation. It allowed to analyze the differences between the two methods in more detail. The calculations of the outgoing slant path radiation exhibited a qualitative agreement of the two methods. However, the SPbSU model - ABC method - gives the larger LM effect in the wing range of the Q-branch and the smaller LM effect in the range of the Q-branch center for all tangent heights as compared to the IMK method. Under strong CO_2 absorption, the values of the LM effect calculated by the two methods differ by a factor of 2 in the Q-branch wing. Differences of the outgoing radiation values calculated by the two methods in some cases reach about $4\text{ mW}/(\text{m}^2\text{ sr cm}^{-1})$.

Table of contents

1. Introduction	1
2. Comparison of the calculations and laboratory measurements of the CO₂ transmittance functions	2
2.1. Description of the experimental data available and the structure of the absorption spectrum in the measurement range	2
2.2. Comparison of the calculated and measured transmittances	4
2.3. Analysis of the experimental spectra and development of the calculation method	4
2.4. Analysis of the calculation results obtained in the range of the LM effect	9
2.5. Summary	11
3. Comparison of the atmospheric radiation and transmittance calculations performed by the two methods	15
3.1. Calculation details and comparison	15
3.2. Comparison of the LME values calculated by the two methods	21
3.3. Summary	29
4. Conclusions	30
5. References	30

List of figures

- Fig. 1.** Lines in the spectral range near 2093 cm^{-1} . 8-1 and 14-2 CO_2 bands.
- Fig. 2.** Lines in the spectral range near 2093 cm^{-1} . 8-1 band of CO_2 .
- Fig. 3.** Lines in the spectral range near 2093 cm^{-1} . 14-2 band of CO_2 .
- Fig. 4a.** Comparison of the measured and calculated (CO_2 spectral lines only) spectra of CO_2 .
- Fig. 4b.** Comparison of the measured and calculated (CO_2 spectral lines only) spectra of CO_2 in N_2 .
- Fig. 5.** H_2O absorption lines in the measurement spectral region.
- Fig. 6.** CO absorption lines in the measurement spectral region.
- Fig. 7a.** Comparison of the measured and calculated (CO_2 , H_2O and CO spectral lines) spectra of CO_2 .
- Fig. 7b.** Comparison of the measured and calculated (CO_2 , H_2O and CO spectral lines) spectra of CO_2 in N_2 .
- Fig. 8a.** Comparison of the CO_2 spectra measured and calculated by fitting (CO_2 , H_2O and CO spectral lines are taken into account).
- Fig. 8b.** Comparison of the spectra of CO_2 in N_2 measured and calculated with fitting (CO_2 , H_2O and CO spectral lines are taken into account).
- Fig. 9a.** Comparison of the measured and calculated (CO_2 , H_2O and CO spectral lines) spectra of CO_2 in the region of the LM effect.
- Fig. 9b.** Comparison of the measured and calculated (CO_2 , H_2O and CO spectral lines) spectra of CO_2 in N_2 in the region of the LM effect.
- Fig. 10a.** Comparison of the measured and calculated (CO_2 , H_2O and CO spectral lines) spectra of CO_2 in the region of the LM effect in an enlarged scale.
- Fig. 10b.** Comparison of the measured and calculated (CO_2 , H_2O and CO spectral lines) spectra of CO_2 in N_2 in the region of the LM effect in an enlarged scale.
- Fig. 10c.** Differences between the transmittances calculated (by SPbSU or IMK methods) using the full or local calibrations and the measurements. CO_2 spectrum.
- Fig. 11.** Q-branch of the CO_2 5-2 transition.
- Fig. 12.** Comparison of the slant path transmittances calculated by the two methods without taking into account the LM effect. Tangent height is 30 km.
- Fig. 13.** Comparison of the slant path transmittances calculated by the two methods without taking into account the LM effect. Tangent height is 20 km.
- Fig. 14.** Comparison of the slant path radiances calculated by the two methods without taking into account the LM effect. Tangent height is 6 km.

- Fig. 15.** Comparison of the slant path radiances calculated by the two methods without taking into account the LM effect. Tangent height is 17 km.
- Fig. 16.** Comparison of the slant path radiances calculated by the two methods without taking into account the LM effect. Tangent height is 30 km.
- Fig. 17a.** Comparison of the slant path radiances calculated with and without LM accounting by the IMK computer code. Tangent height is 17 km.
- Fig. 17b.** Comparison of the slant path radiances calculated with and without LM accounting by the SPbSU computer code. Tangent height is 17 km.
- Fig. 18.** Comparison of Line Mixing Effects calculated by the two methods. Tangent height is 6 km.
- Fig. 19.** Comparison of Line Mixing Effects calculated by the two methods. Tangent height is 8 km.
- Fig. 20.** Comparison of Line Mixing Effects calculated by the two methods. Tangent height is 11 km.
- Fig. 21.** Comparison of Line Mixing Effects calculated by the two methods. Tangent height is 14 km.
- Fig. 22.** Comparison of Line Mixing Effects calculated by the two methods. Tangent height is 17 km.
- Fig. 23.** Comparison of Line Mixing Effects calculated by the two methods. Tangent height is 20 km.
- Fig. 24.** Comparison of Line Mixing Effects calculated by the two methods. Tangent height is 23 km.
- Fig. 25.** Comparison of Line Mixing Effects calculated by the two methods. Tangent height is 25 km.
- Fig. 26.** Comparison of Line Mixing Effects calculated by the two methods. Tangent height is 30 km.
- Fig. 27.** Comparison of Line Mixing Effects calculated by the two methods. Tangent height is 35 km.
- Fig. 28.** Comparison of the spectra calculated with and without applying the χ - factor to the P- and R-branch lines by the IMK code. The Q-branch LM is taken into account, tangent height is 17 km.
- Fig. 29.** Comparison of spectra calculated with Q-branch LM and applying the χ - factor to P- and R- branch lines, and without both, respectively. Both spectra were calculated by the IMK code; tangent height is 17 km.
- Fig. 30.** Comparison of the spectra calculated with PR-branch χ - factor and Q-branch LM and with taking the PQR-branch LM into account, respectively. Tangent height is 17 km. Both spectra were calculated by the IMK code.

1. Introduction

High requirements with regard to the accuracy and vertical resolution of atmospheric component retrieval and the necessity to extend the list of retrieved parameters led to a new generation of devices with enhanced radiometric characteristics. Progress in the methods of sounding the atmospheric state and composition calls for developing more detailed and accurate computer codes modeling the atmospheric radiation and, hence, more perfect computations of the variables measured by spectral devices - atmospheric radiance and transmittance. In particular, interpretation of the measurement data of the MIPAS spectrometer [Endemann et al., 1997] developed at the IMK FZK and its excellent characteristics - a small measurement error and high spectral resolution - requires a relevant high level of calculation accuracy. As known, the phenomenon of spectral absorption line coupling, (generally called line mixing) essentially influences the radiation transfer in the IR spectral range used in the MIPAS measurements and especially in the $15\mu\text{m}$ band of CO_2 . The physical nature of this phenomenon has been widely described in scientific literature. Therefore, attention shall be restricted to comparing the experimental laboratory spectra with the calculations and the outgoing slant path radiance values calculated by two methods of taking the Line Mixing (LM) into account.

One of these methods is applied at the IMK. It models the complex relaxation matrix by applying the Exponential Power Gap Law as introduced by Strow et al. [Strow et al., 1994]. The parameters of the exponential power gap law are determined by fitting the diagonal elements of the relaxation matrix to the sum rule within which the rotational state-to-state cross-sections determine the relaxation matrix elements. The model is described in detail in [Funke et al., 1997]. Although up to now the approach is limited to Q-branch line-mixing, the transfer of transition probability from the Q- to the P - and R-branch lines is considered within the model.

The other method is referred to as the ABC (Adjusted Branch Coupling) method. It was originally developed by M.V. Tonkov and N.N. Filippov [Tonkov et al., 1996] and used for atmospheric applications at the SPbSU. This new empirical method of band shape calculation taking into account the LM effect is based on a strong collision model with weakened interbranch coupling. The P, Q and R branches corresponding to one vibration quantum transition are considered simultaneously. Only one parameter defining the power of the branch interaction is used for each specific gas. This parameter depends on the perturbing gas type and is the same for all IR absorption bands of a molecule. The value of this parameter was determined for CO_2 on the basis of the known experimental data of laboratory measurements at the wings of the $4.3\mu\text{m}$ band of CO_2 . It is very important that no additional information except for that contained in the existing spectral databases is required in the calculations using the ABC method. A detailed description of the method was also given by [Hollweg et al., 1995].

As mentioned above, the main objective of this study is to compare the results obtained for the LM effect by different methods. At first, let us consider the simplest case of transmittance function measurements under controlled laboratory conditions.

2. Comparison of the calculations and laboratory measurements of the CO₂ transmittance functions

2.1. Description of the experimental data available and the structure of the absorption spectrum in the measurement range

Two laboratory spectra of the transmittance functions were provided by F. Rachet, Laboratoire de Physique Moléculaire, Paris [Valentin and Rachet, 1995].

One represents the absorption spectrum of pure CO₂ and the other is the spectrum of CO₂ in N₂ measured in the gas absorption cell under controlled conditions. The measurements were carried out in the 2085 - 2098 cm⁻¹ spectral range. It is known that these spectra need an additional calibration - it is necessary to define more correctly the scale and zero shift of the measured values. Precise information on measurement spectral resolution is lacking, but it is known that it is very high, and this allows to compare these measurements with the monochromatic calculations.

Let us analyze the structure of the spectra in the measurement spectral range using the known HITRAN 92 database. In this spectral range, the main CO₂ isotope absorption takes place in the overlapping vibration - rotation bands due to the transitions of 8-1 and 14-2. (All transition designations correspond to those of the HITRAN 92 database [Rothman et al., 1992].) Maximum CO₂ absorption is observed near 2093.4 cm⁻¹ in the region of the 14-2 Q-branch. The absorption lines of the R-branch of the 8-1 band of CO₂ can also be noticed in this spectral range. The positions and intensities of these absorption bands are represented graphically in Figs. 1-3.

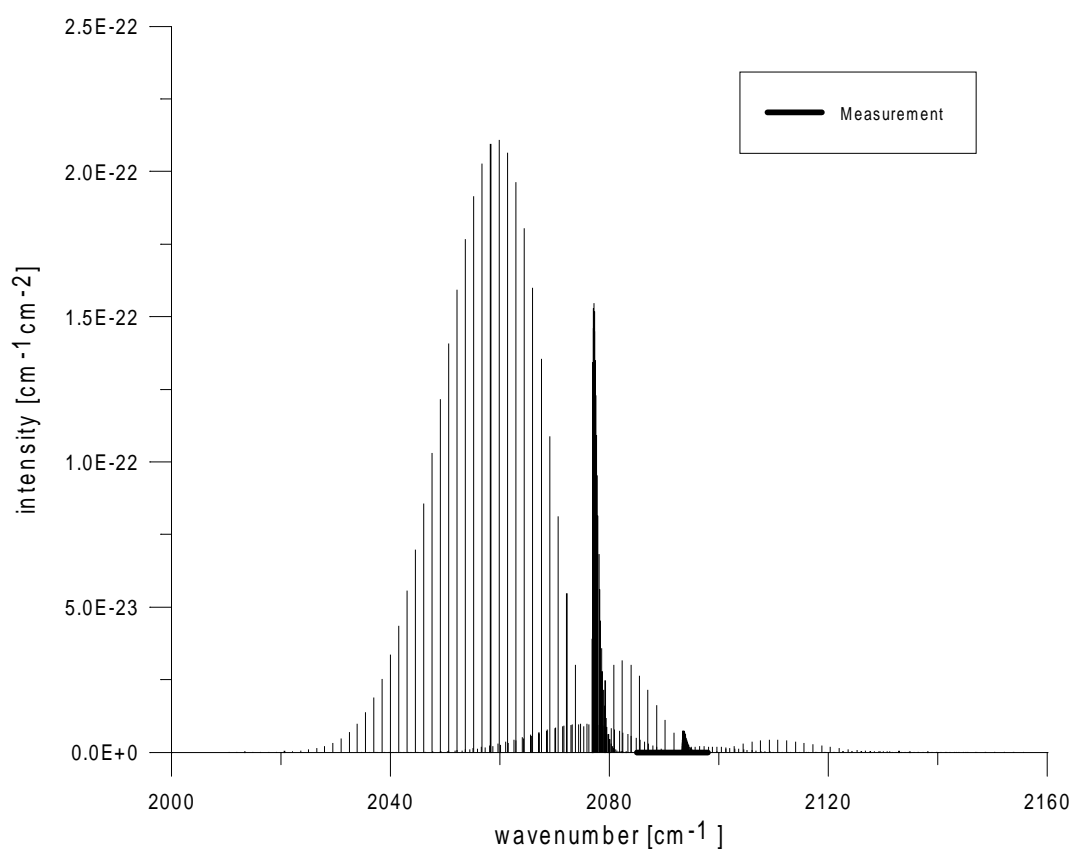


Fig. 1. Lines in the spectral range near 2093 cm⁻¹. 8-1 and 14-2 CO₂ bands.

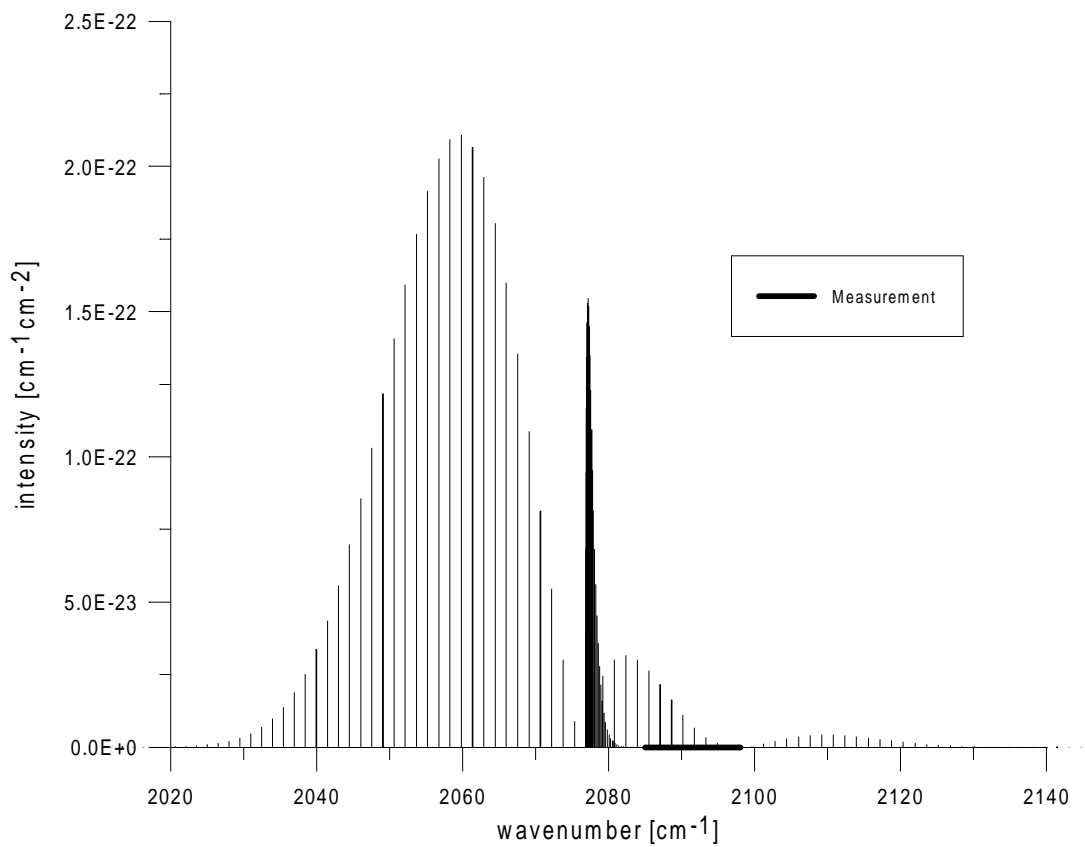


Fig. 2. Lines in the spectral range near 2093 cm⁻¹. 8-1 band of CO₂.

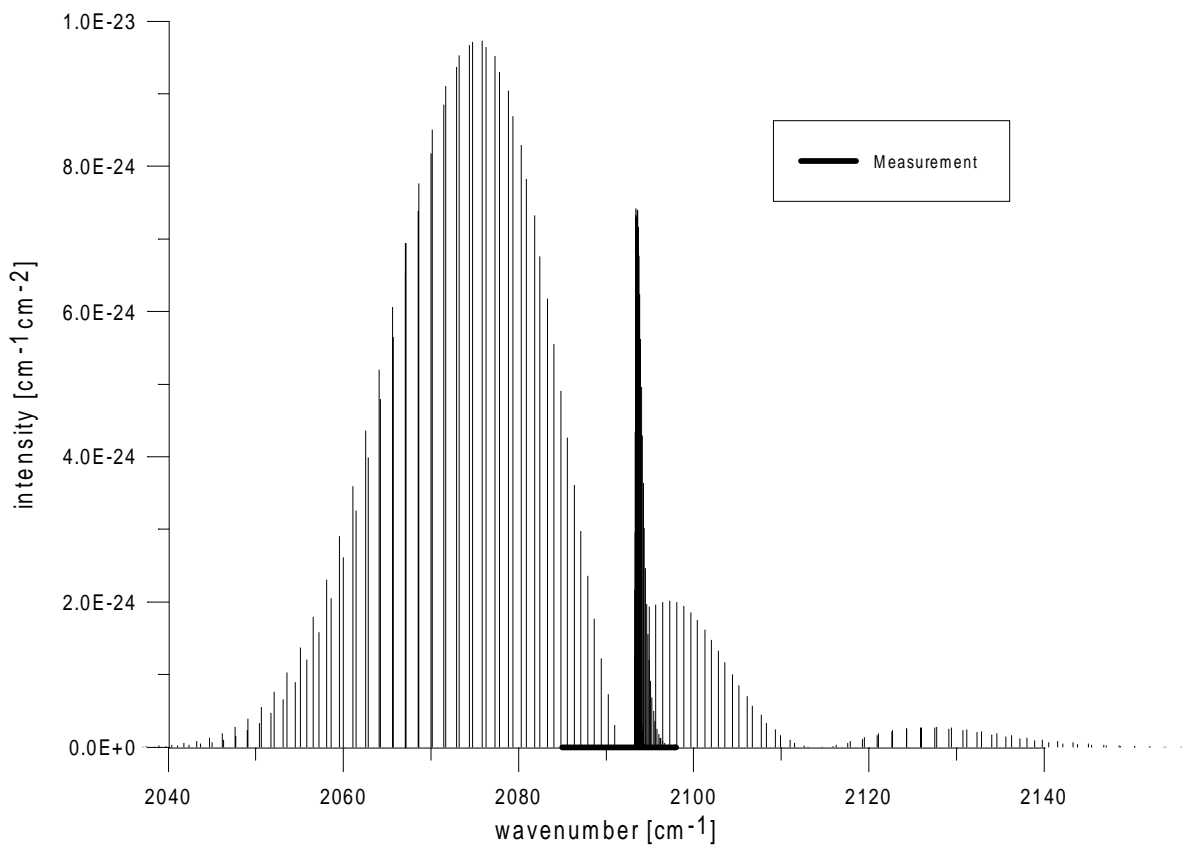


Fig. 3. Lines in the spectral range near 2093 cm⁻¹. 14-2 band of CO₂.

2.2. Comparison of the calculated and measured transmittances

As the main objective of the study consists in comparing the calculation methods of the LM effect, the work was performed as follows. At first, after identifying all causes of discrepancies, we reached an agreement of the calculated and measured values in all spectral ranges with the exception of the interval where the LM effect occurs. Then, the LM calculations were compared with each other using the approved calculation and calibration procedure outlined in Section 2.3.

2.3. Analysis of the experimental spectra and development of the calculation method

To analyze the experimental spectra, both computer codes (IMK and SPbSU) were applied. It should be noted that the transmittances calculated by the two computer codes developed independently at the SPbSU and IMK without taking the LM into account differ by less than 0.001 of transmittance. The calculations taking into account the LM effect also practically agree, except for the range of LM influence, of course.

The results of the comparison of the CO₂ absorption spectra calculated for pure CO₂ and CO₂ in N₂ are presented in Figs. 4a and 4b, respectively. (It must be emphasized that all figures in this Section illustrating the comparisons of calculated and measured transmittances are drawn in the same manner: the transmittance spectra are represented at the top with the measured spectra indicated by the bold curve, while the differences between the calculated and measured transmittances are shown in the lower part.)

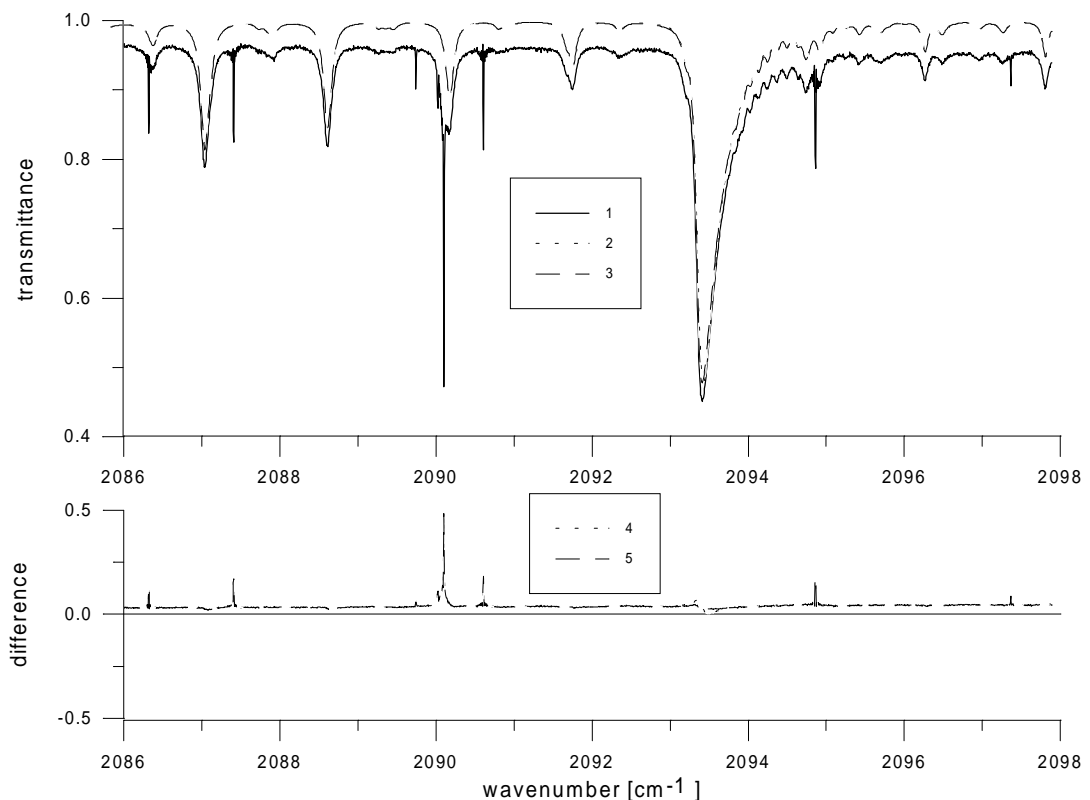


Fig. 4a. Comparison of the measured and calculated (CO₂ spectral lines only) spectra of CO₂.

1 - measured transmittance spectrum; 2,3 - transmittance spectra calculated by SPbSU and IMK methods, respectively; 4,5 - differences between the transmittances calculated by SPbSU or IMK methods and the measurements, respectively.

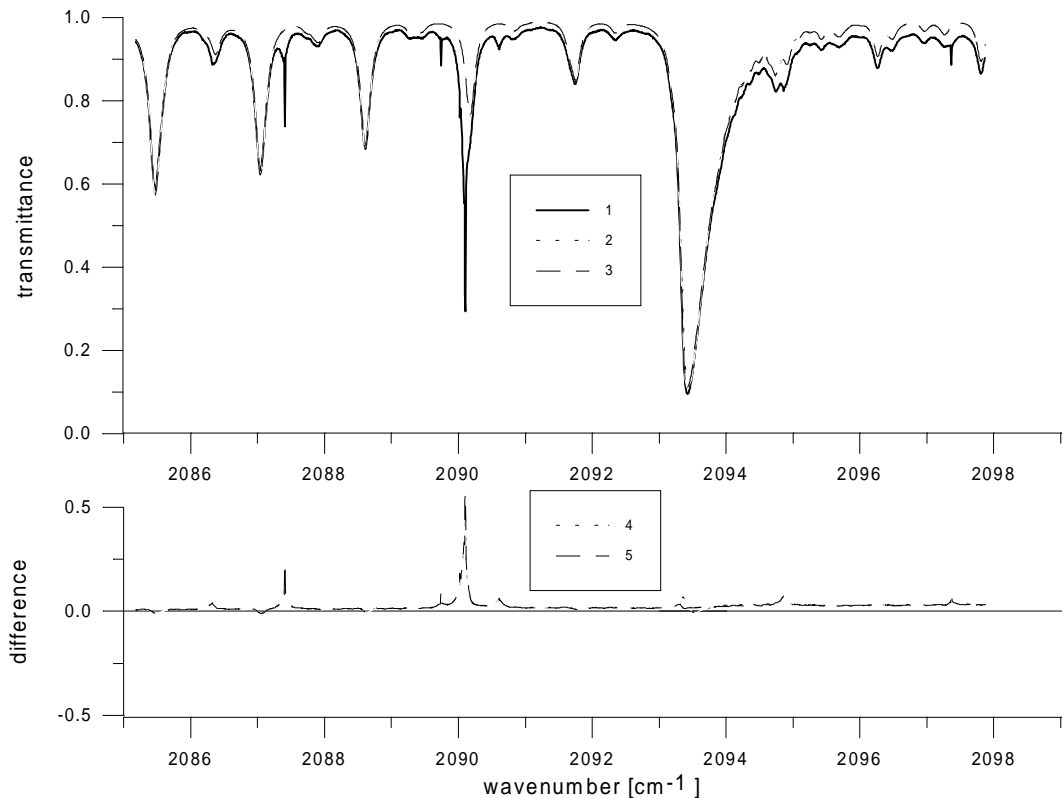


Fig. 4b. Comparison of the measured and calculated (CO₂ spectral lines only) spectra of CO₂ in N₂.

1 - measured transmittance spectrum; 2,3 - transmittance spectra calculated by SPbSU and IMK methods, respectively; 4,5 - differences between the transmittances calculated by SPbSU or IMK methods and the measurements, respectively.

The systematic discrepancy between the calculated and measured spectra which is caused by the normalization uncertainty of the experimental spectra is obvious from Figs. 4a and 4b. In addition, other absorption lines apart from those of CO₂ are observed in the measured spectrum. According to the HITRAN 92 database, the absorption lines of water vapor, ozone, N₂O, CO, CH₄ and a number of other atmospheric trace gases exist in the spectral range examined. By transmittance calculation and comparison of the lines in the measured spectra with those of the HITRAN 92 database, it was found out that all lines observed have to be attributed to H₂O and CO. In Figs. 5 and 6 the absorption line positions and intensities of the above gases are plotted for the examined spectral range. The approximate concentrations of these two gases have been determined by a fitting procedure and applied in further calculations.

In addition to the H₂O absorption lines broadened by the pressure of about 1 atm, narrow lines (which are the same in terms of position and intensity, but at a small - not exceeding several millibars - pressure) are found in the measured spectrum of CO₂ in N₂. Their existence is supposed to be caused by the measurement device which contains H₂O at a small pressure. In the measured spectrum of CO₂, similar narrow CO lines are observed.

As these additional CO and H₂O lines are very narrow (not more than three measurement points in the measured spectrum) and information on the pressure and temperature of the respective gases is lacking, the measurements of these points were replaced by the values interpolated from the nearest measurements.

A good fit of the calculated spectra to the measured one has been achieved by displacing the H₂O line near 2090 cm⁻¹ by 0.015 cm⁻¹. Such a displacement of the line is assumed to be caused by the known line-shift effect or the HITRAN 92 data error.

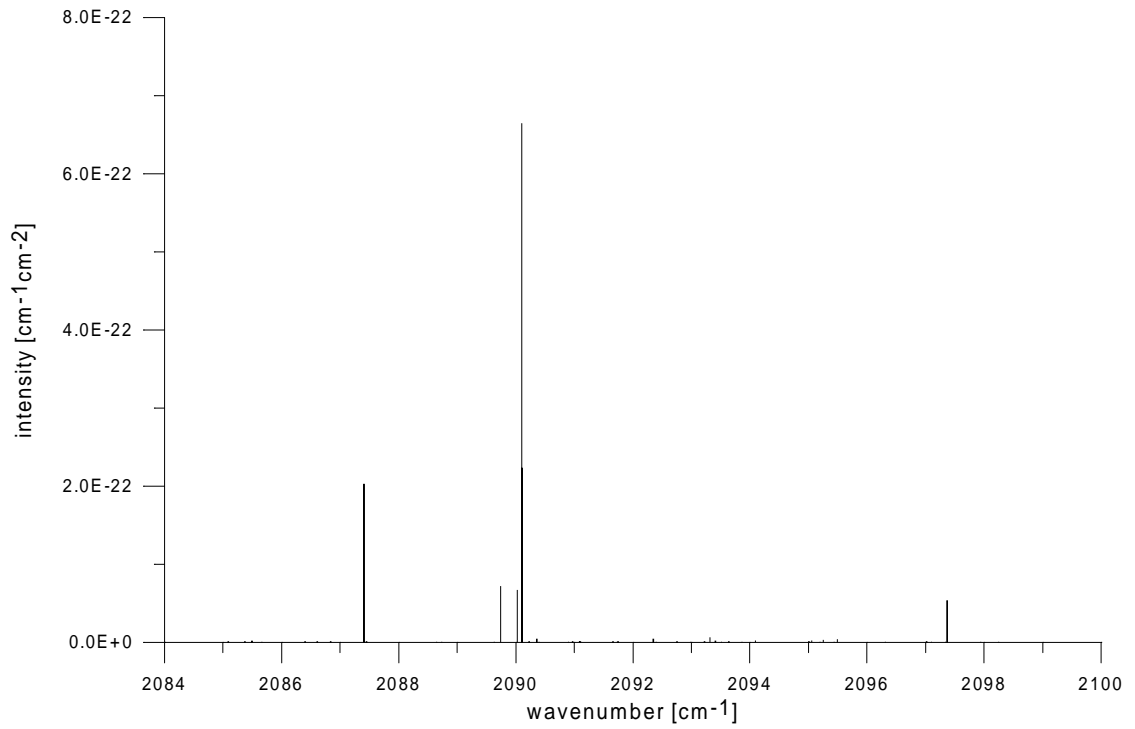


Fig. 5. H₂O absorption lines in the measurement spectral region.

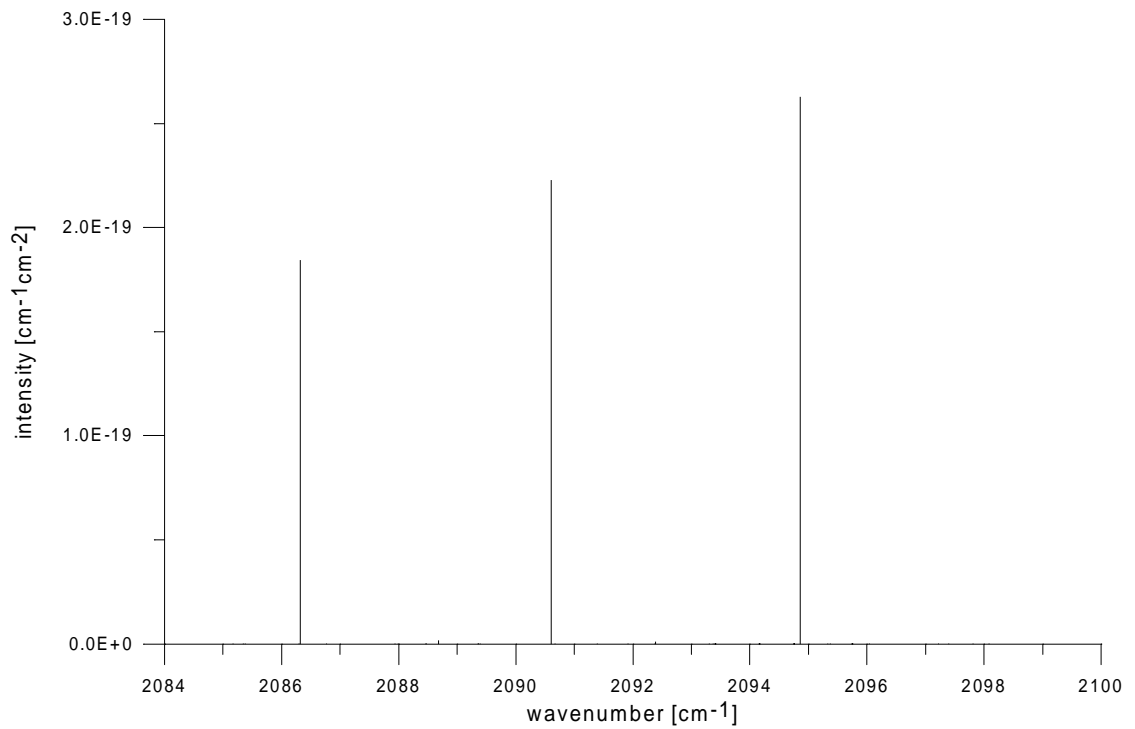


Fig. 6. CO absorption lines in the measurement spectral region.

Based on the above measurement spectra analysis, the transmittance spectra in the examined spectral range were calculated taking into account H₂O and CO absorption.

In Figs. 7a, 7b, the calculated and measured transmittance spectra are compared. In these figures, the H₂O and CO lines at a small pressure are eliminated from the measured spectra.

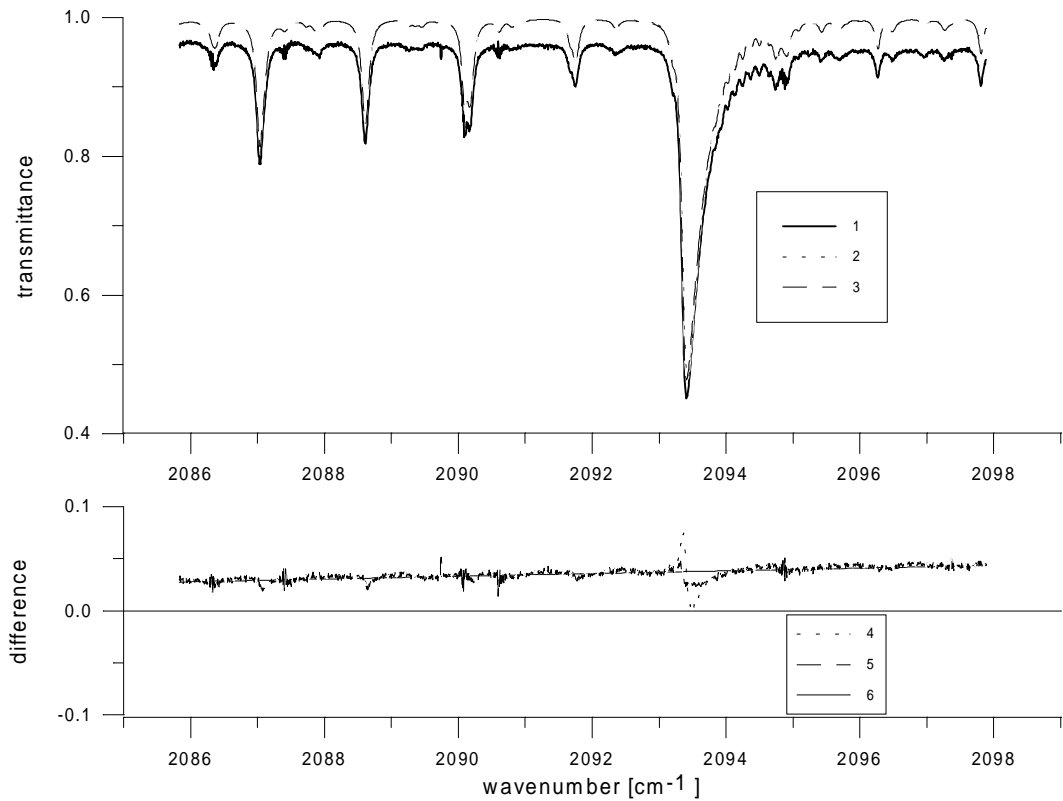


Fig. 7a. Comparison of the measured and calculated (CO_2 , H_2O and CO spectral lines) spectra of CO_2 .

1 - measured transmittance spectrum; 2,3 - transmittance spectra calculated by SPbSU and IMK methods, respectively; 4,5 - differences between the transmittances calculated by SPbSU or IMK methods and the measurements, respectively; 6 - linear fitting of curve 4.

It must be noted that the Y-scale in the lower part of Figs. 7a and 7b has been increased by a factor of 5 as compared to Figs. 4a and 4b.

It is evident from Fig. 7 that the differences between the measured and calculated values, which had been caused by neglecting the CO and H_2O lines, are considerably decreased. The slope of the measured spectra clearly visible in Fig. 7 is most likely due to either a weak selective attenuation or the experimental conditions. This is confirmed by curve 6 which represents the linear fitting of the differences between the calculated and measured transmittances. In Fig. 7, significant deviations of the calculations and measurements are found at the origins of the CO_2 8-1 band of the R-branch. These deviations may result from many reasons: errors when specifying the experimental conditions (pressure, temperature, gas content) or line structure parameters (line intensity and half-width) and errors of experimental data calibration. Unfortunately, information is not sufficient to compensate these deviations.

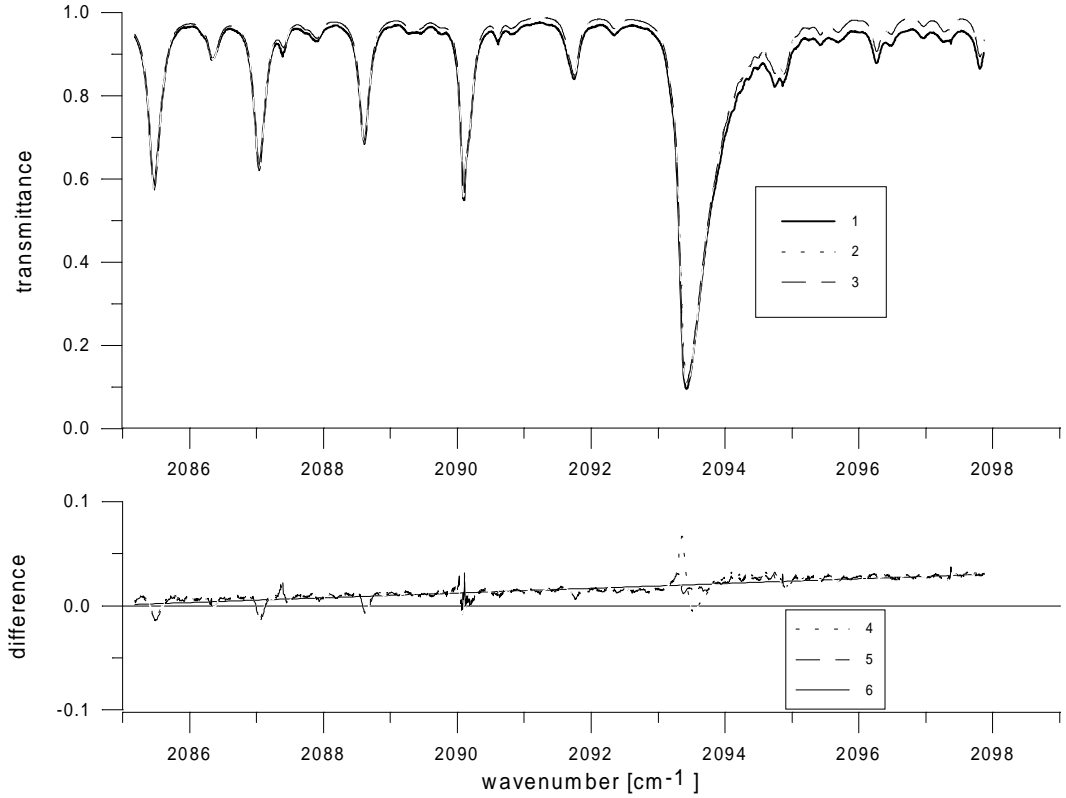


Fig. 7b. Comparison of the measured and calculated (CO_2 , H_2O and CO spectral lines) spectra of CO_2 in N_2 .

1 - measured transmittance spectrum; 2,3 - transmittance spectra calculated by SPbSU and IMK methods, respectively; 4,5 - differences between the transmittances calculated by SPbSU or IMK methods and the measurements, respectively; 6 - linear fitting of curve 4.

For the calculation results presented in Figs. 7a and 7b, fitting was performed on the basis of the following formula:

$$\min_{k,u} \sum_i ((P_i^c \cdot (k + r \cdot w_i) + u) - P_i^m)^2 \quad (1)$$

where P_i^c and P_i^m are the calculated and measured transmittances, respectively; w_i is the wavenumber; k, r, u are the fitting parameters. Fitting is carried out in all measurement spectral ranges with the exception of the $2091\text{-}2095 \text{ cm}^{-1}$ interval, where the transmittance is essentially affected by the LM effect.

In Figs. 8a and 8b, the results of fitting the measured and calculated transmittance spectra are given. It is obvious that the differences between the calculation and experiment are 0.02-0.03 of the transmittance only for the CO_2 and H_2O lines, and less than 0.01 of transmittance in the remaining cases. (It should be mentioned that the $2091\text{-}2095 \text{ cm}^{-1}$ interval, where the LM effect becomes apparent, is still not discussed.) Apparently, a better agreement of calculated and measured data cannot be achieved with the information available.

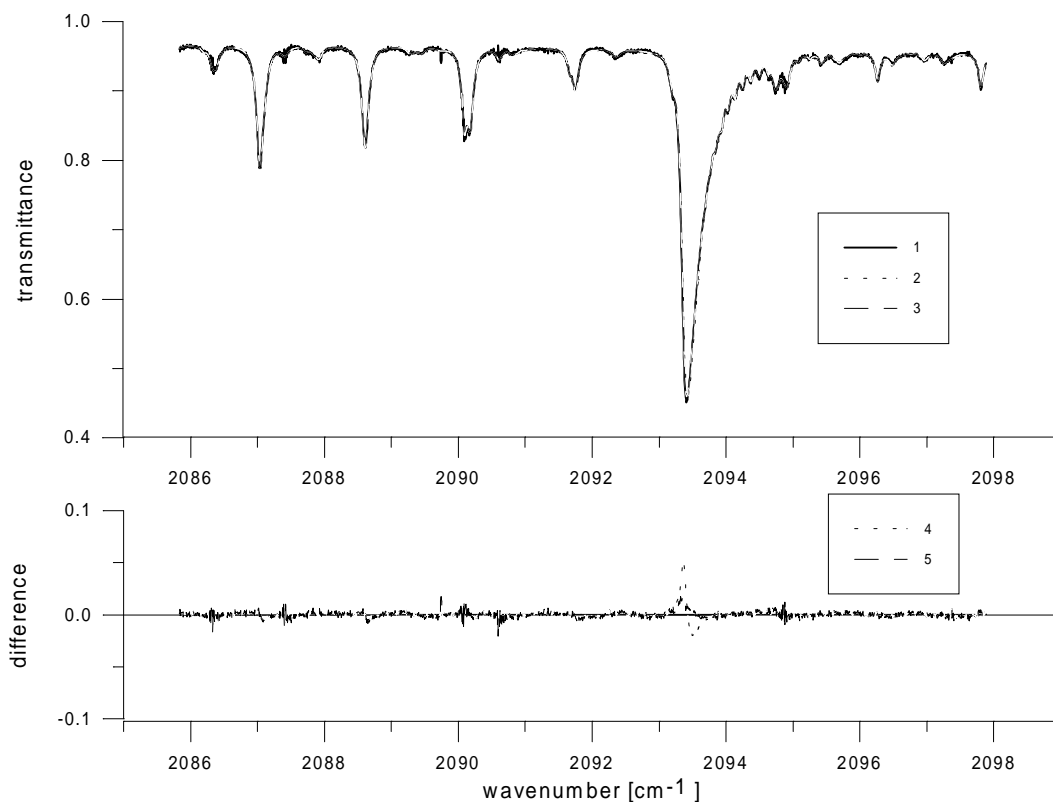


Fig. 8a. Comparison of the CO₂ spectra measured and calculated by fitting (CO₂, H₂O and CO spectral lines are taken into account).

1 - measured transmittance spectrum; 2,3 - transmittance spectra calculated by SPbSU and IMK methods, respectively; 4,5 -differences between the transmittances calculated by SPbSU or IMK methods and the measurements, respectively.

2.4. Analysis of the calculation results obtained in the range of the LM effect

In Figs. 9a and 9b, the transmittance functions calculated taking into account the LM effect by the SPbSU and IMK codes are given. The transmittance spectrum calculated with neglecting the LM effect is also indicated for comparison. As mentioned above the data calculated by both above codes neglecting the LM effect are in good agreement. Both results obtained taking the LM effect into account describe the tendency of the LM influence on the transmittance functions correctly. However, they differ by up to 0.05 of transmittance in the narrow spectral range of maximum absorption. In the region of the long-wave wing of the Q-branch, both methods of LM accounting practically yield congruent results. The data calculated by the two methods differ slightly in the region of the short-wave wing.

For analyzing the behavior of the examined curves in the region of the Q-branch, let us examine Figs. 10a and 10b which represent the section corresponding to the absorption maximum in Figs. 9a,b in an enlarged scale. The differences between the experimental data and those calculated by the IMK method do not exceed 0.02 of transmittance and reach a maximum in the region of maximum curve slope. At the same time, the differences between the experimental data and those calculated by the SPbSU method are considerably greater and reach about 0.06 of the transmittance even in the narrow spectral range. It can be seen from Figs. 10a and 10b that such a large discrepancy results from the absorption maximum dislocation in the SPbSU calculation, which is equal to 0.02-0.03 cm⁻¹ in the short-wave spectral range. These discrepancies cannot be explained by the calibration errors (i. e. by the inaccuracy in determining the parameters k, r, u of the formula (1)). It was tested as follows. The local calibration for both calculations was applied only in the 2093-2094 cm⁻¹ spectral interval. The transmittance differences due to the use of various calibrations were no more than 0.005 and 0.01 of the transmittance for the IMK and SPbSU methods, respectively. The comparison of

the transmittances calculated using the local and full (over the entire measurement region except the 2091-2095 cm^{-1} spectral interval) calibrations is presented in Fig. 10c.

The residual discrepancies between the measured and calculated data are reduced by a factor of 2 by the SPbSU model as compared to the simulation disregarding the line-mixing effects, and by a factor of 5 by the IMK model. Both residual spectra, however, are still characterized by two systematic deviations which obviously are above the noise level.

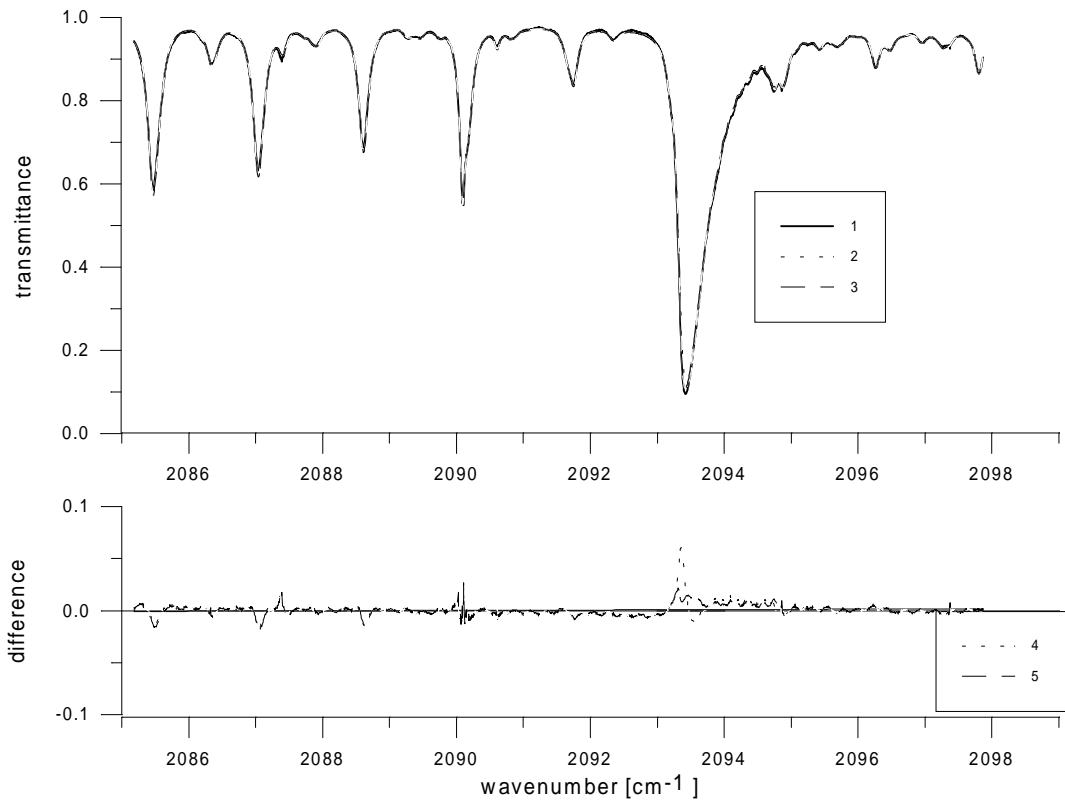


Fig. 8b. Comparison of the spectra of CO_2 in N_2 measured and calculated with fitting (CO_2 , H_2O and CO spectral lines are taken into account).

1 - measured transmittance spectrum; 2,3 - transmittance spectra calculated by SPbSU and IMK methods, respectively; 4,5 - differences between the transmittances calculated by SPbSU or IMK methods and the measurements, respectively.

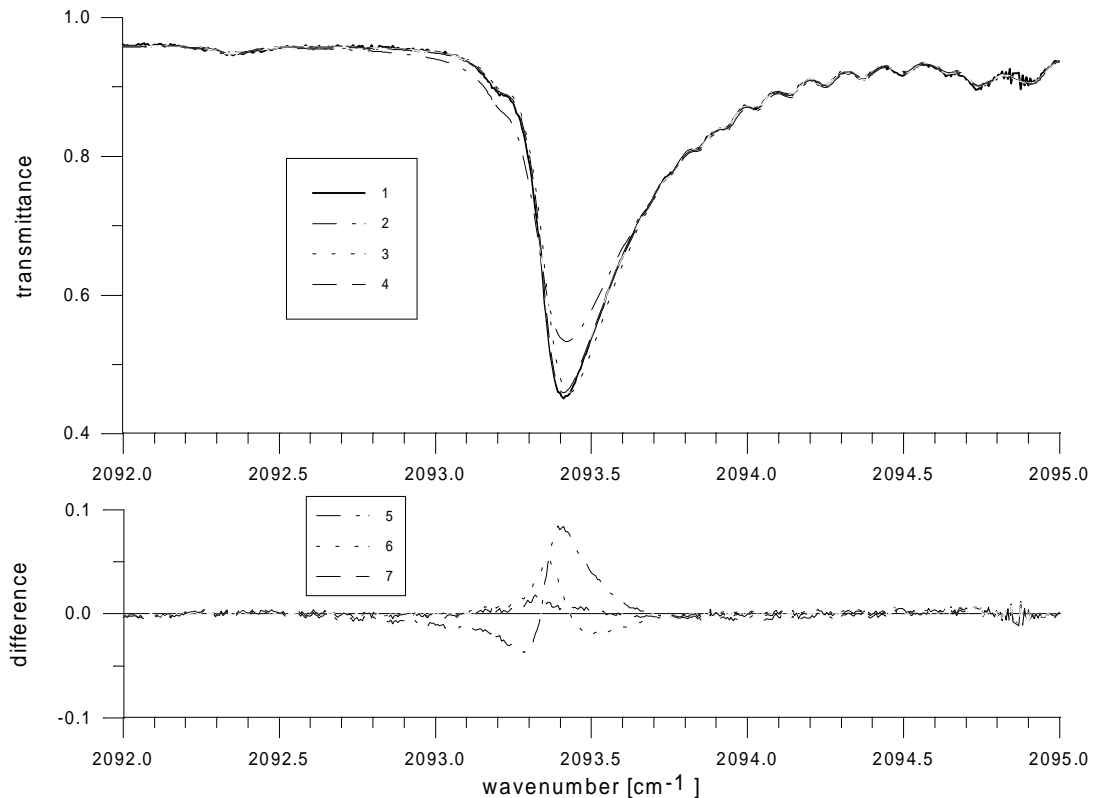


Fig. 9a. Comparison of the measured and calculated (CO_2 , H_2O and CO spectral lines) spectra of CO_2 in the region of the LM effect.

1 - measured transmittance spectrum; 2 - transmittance spectrum calculated without LM; 3,4 - transmittance spectra calculated with LM by SPbSU and IMK methods, respectively; 5 - differences between the transmittances calculated without LM and the measurements; 6,7 - differences between the transmittances calculated with LM by SPbSU or IMK methods and the measurements, respectively.

2.5. Summary

The following conclusions can be drawn from the comparison of the transmittance calculations obtained using the two methods taking into account the Line Mixing effect with the laboratory measurements:

- Both methods provide a correct qualitative description of the Line Mixing effect.
- In the region of the Q-branch wings, the results of both methods nearly agree with each other. In the low-frequency vicinity of the Q-branch, both methods yield practically coincident results.
- In the region of the Q-branch center, the IMK method considers the LM effect better than the SPbSU model. The maximum residual discrepancies between the calculated and measured results are about 0.02 and 0.06 of the transmittance for the IMK and SPbSU models, respectively.
- In the high-frequency vicinity of the Q-branch, the residual differences for both models are comparable in magnitude (less than 0.02 transmittance), but different in sign.
- The larger residual discrepancies between measured and calculated data in the region of the Q-branch center for the SPbSU model show characteristics of an absorption maximum shift. Most likely, such shift is a feature of this method.

It should be emphasized that the above conclusions are made on the basis of the comparison of two methods only for two experimental spectra and one vibration transition. For a more detailed and justified

analysis, it is necessary to compare the statistically reliable data sets in different spectral ranges and under various measurement conditions.

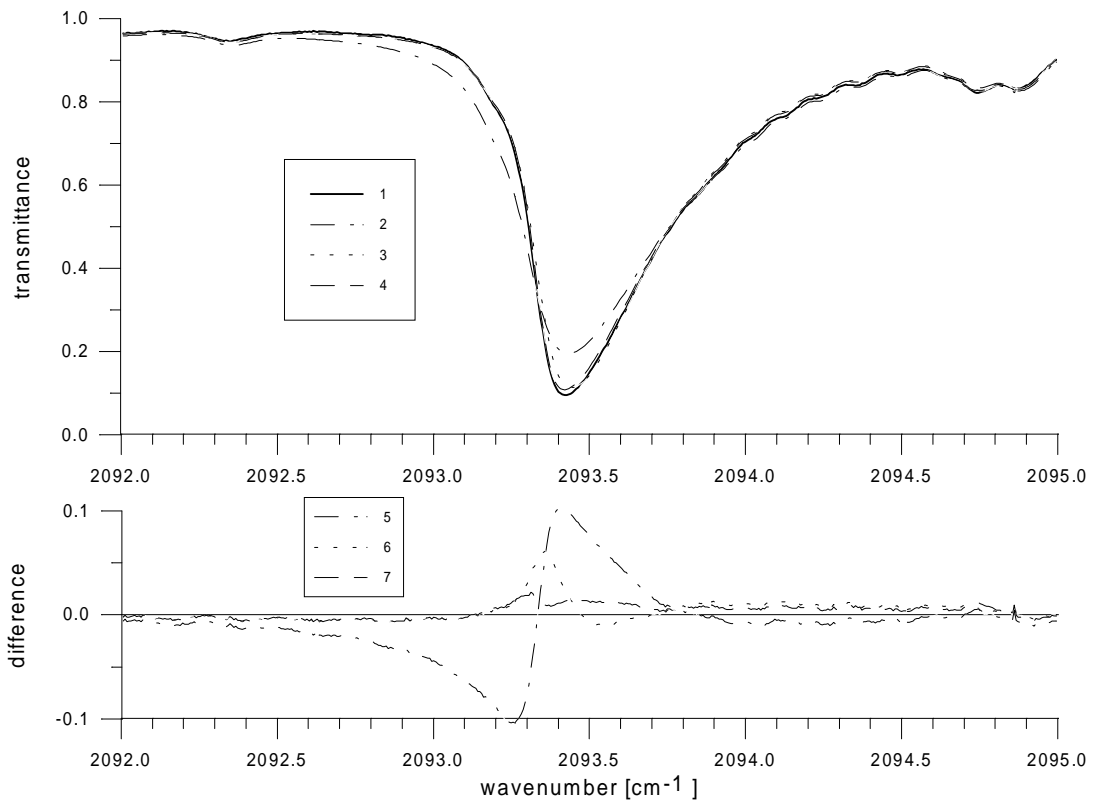


Fig. 9b. Comparison of the measured and calculated (CO_2 , H_2O and CO spectral lines) spectra of CO_2 in N_2 in the region of the LM effect.

1 - measured transmittance spectrum; 2 - transmittance spectrum calculated without LM; 3,4 - transmittance spectra calculated with LM by SPbSU and IMK methods, respectively; 5 - differences between the transmittances calculated without LM and the measurements; 6,7 - differences between the transmittances calculated with LM by SPbSU or IMK methods and the measurements, respectively.

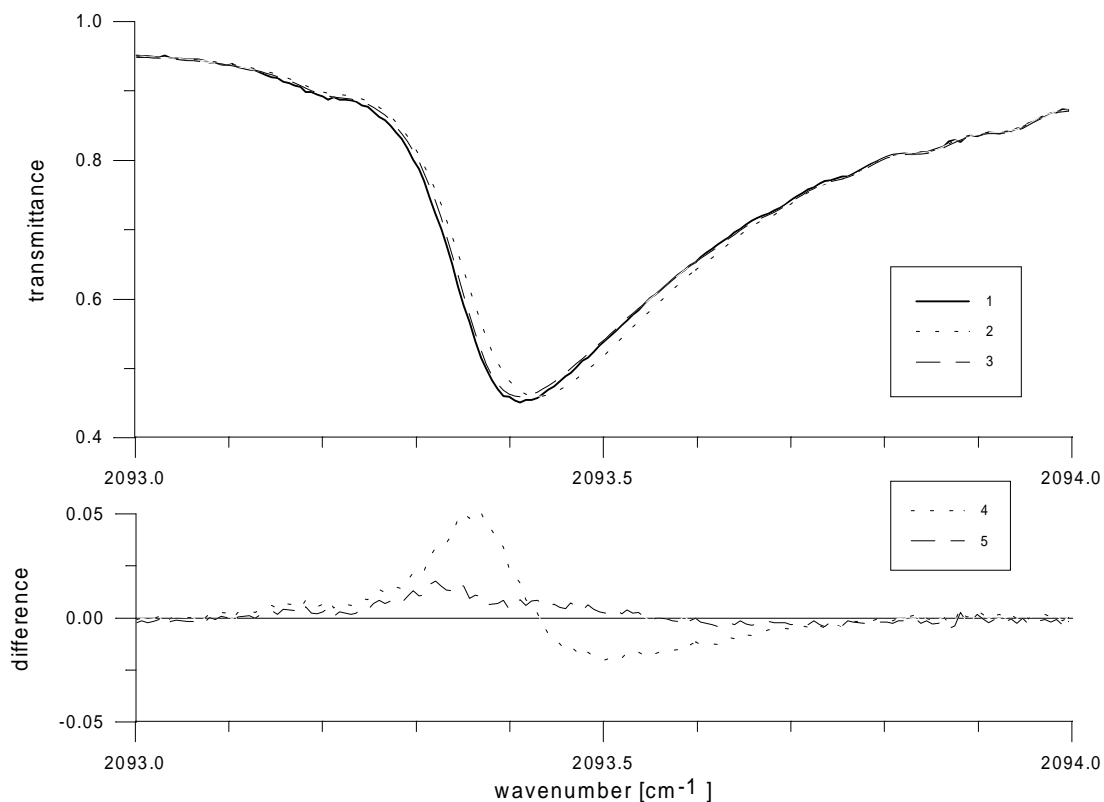


Fig. 10a. Comparison of the measured and calculated (CO_2 , H_2O and CO spectral lines) spectra of CO_2 in the region of the LM effect in an enlarged scale.

1 - measured transmittance spectrum; 2,3 - transmittance spectra calculated with LM by SPbSU and IMK methods, respectively; 4,5 - differences between the transmittances calculated by SPbSU or IMK methods and the measurements, respectively.

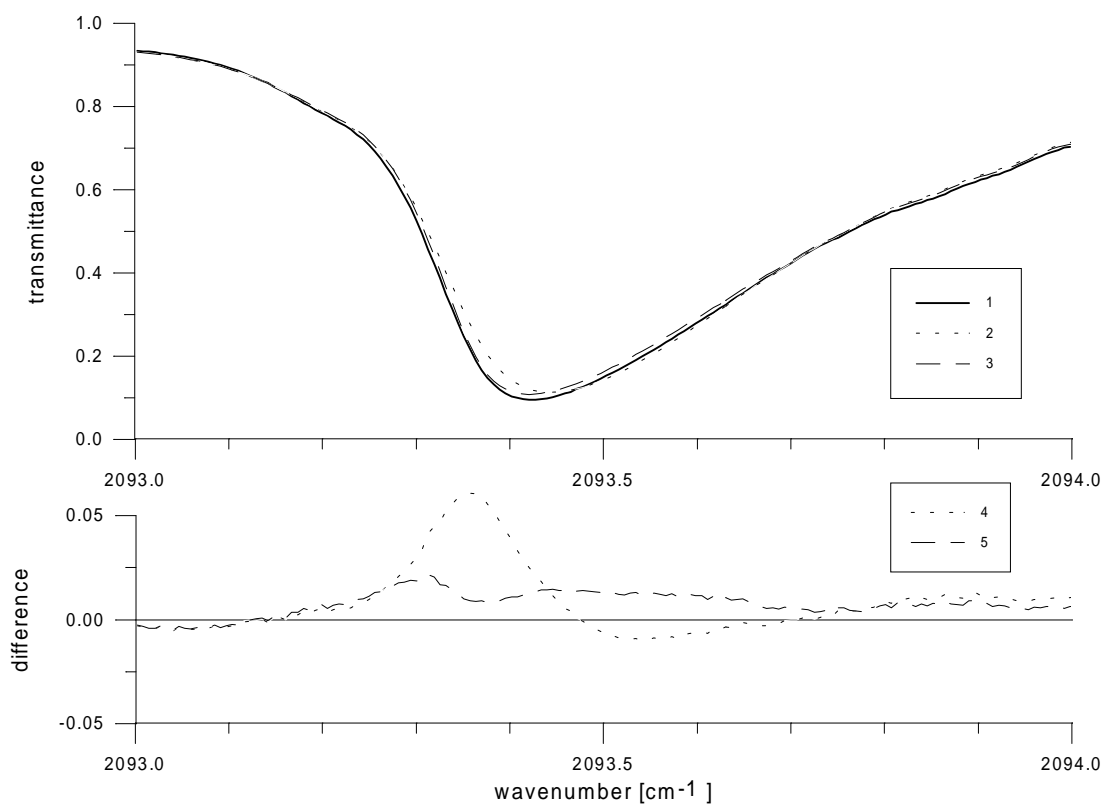


Fig. 10b. Comparison of the measured and calculated (CO_2 , H_2O and CO spectral lines) spectra of CO_2 in N_2 in the region of the LM effect in an enlarged scale.

1 - measured transmittance spectrum; 2, 3 - transmittance spectra calculated with LM by SPbSU and IMK methods, respectively; 4,5 - differences between the transmittances calculated by SPbSU or IMK methods and the measurements, respectively.

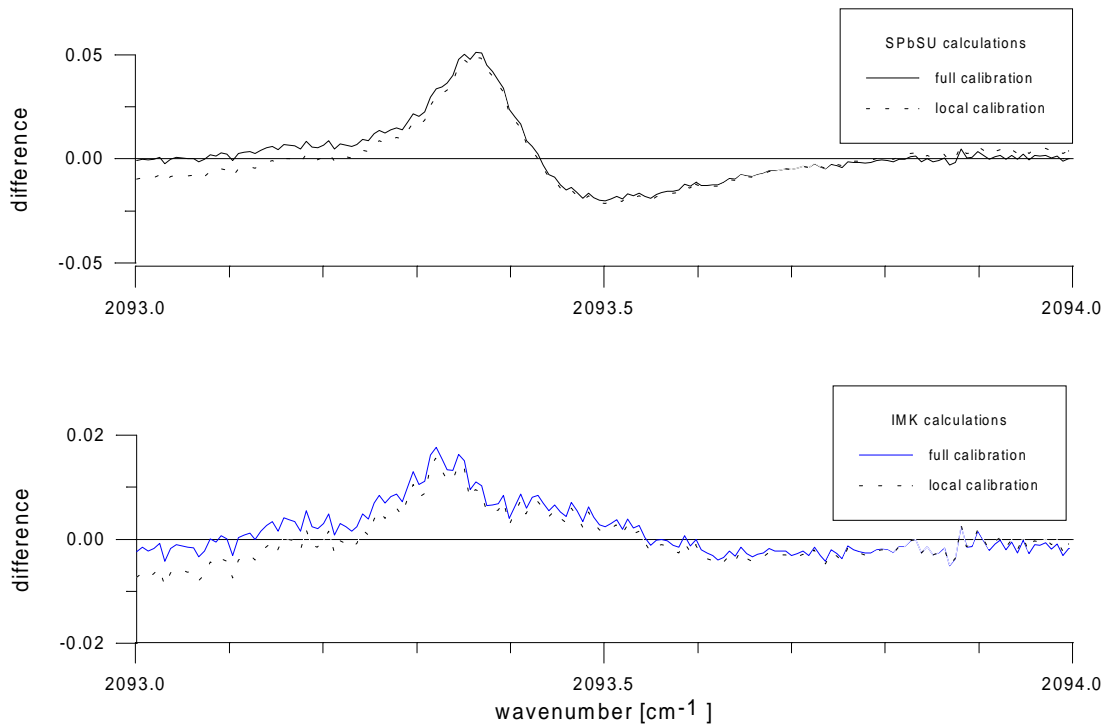


Fig. 10c. Differences between the transmittances calculated (by SPbSU or IMK methods) using the full or local calibrations and the measurements. CO_2 spectrum.

3. Comparison of the atmospheric radiation and transmittance calculations performed by the two methods

3.1. Calculation details and comparison

Unfortunately, no experimental information is available on the slant path transmittance or radiance of the atmosphere, for example, from MIPAS. Therefore, the present study is devoted to the comparison of the results obtained by calculations with the two computer codes used in the previous sections:

- a) the IMK code considering the LM effect using the IMK model and
- b) the SPbSU code taking into account the LM effect by the ABC method.

The Q-branch of the 5-2 transition of the main CO₂ isotope near 720 cm⁻¹ was chosen for these comparisons because of the strength of the LM effect observed here. In Fig. 11 the lines of this Q-branch are given in accordance with the HITRAN 92 database. Fig. 11 illustrates the maximum line concentration in the 720.5-720.7 cm⁻¹ spectral interval, where the maximum LM effect is expected. Judging from the Q-branch shape, the maximum LM effect in the band wing at atmospheric pressure can be assumed for wavenumbers greater than 720.8 cm⁻¹.

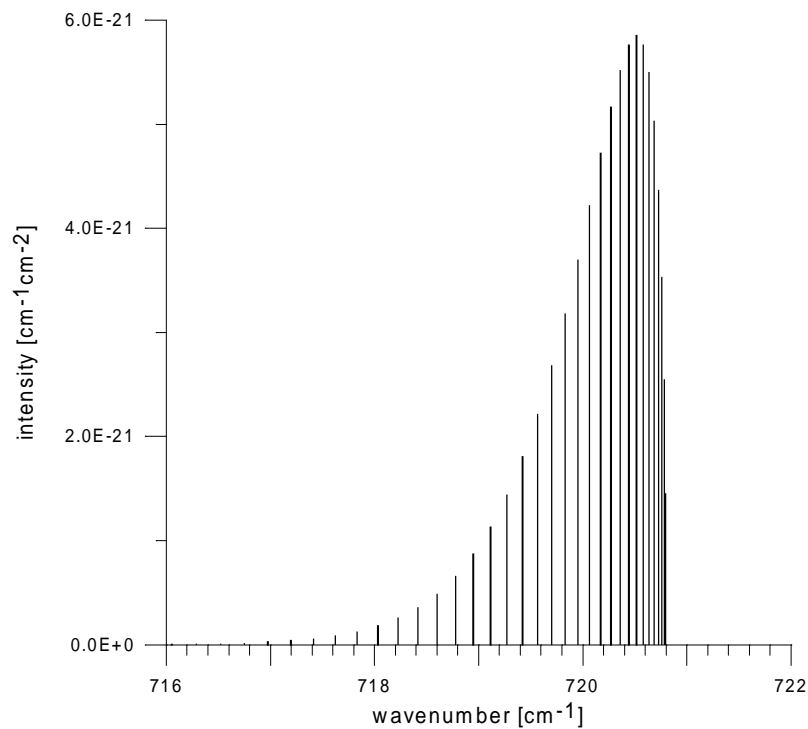


Fig 11. Q-branch of the CO₂ 5-2 transition.

That is why the 719-722 cm⁻¹ interval was chosen for the study. Calculations were carried out for the 6-35 km range of the tangent heights, as the effect of LM on the radiation is not observed at greater tangent heights.

For a more detailed analysis of the differences between the data calculated by the two codes, the monochromatic transmittance and radiance functions were compared. These calculations did not consider additional physical impacts, such as refraction, contributions of interfering species or instrumental line shape effects. When applying MIPAS data on the finite spectral resolution, the calculations by the two codes may give, in a number of cases, results with differences that are much less than the revealed ones.

To compare the methods of LM considering, let us first compare the computer codes as such. For this purpose, atmospheric transmittance and radiation were calculated under special operating conditions excluding the LM effect. The calculations of atmospheric slant path transmittance and radiance are more complicated than those simulating the laboratory measurements of cell gas absorption. Therefore, poor agreement was reached for the two computer codes neglecting the LM effect. This may be attributed to the special features of the used codes. IMK software was developed for interpretation of MIPAS measurements. It takes into account all possible physical impacts influencing the atmospheric radiation transfer. The SPbSU software is designed to study the LM effect. Therefore, it accounts for atmospheric gas absorption taking into account a number of absorption lines. No special methods simplifying the calculations are used.

Let us also notice that in the IMK code the so-called χ - function is used for correcting the overall contribution of the far wings of all CO₂ lines of the respective band. However, the χ - function is only applied to Q-lines more than 10 cm⁻¹ away from the Q-branch center in order not to interfere with a proper Q-branch line mixing modeling. The ABC method of LM accounting applied in the SPbSU code does neither require nor allow the use of the χ - function. The contribution of far band wings is sufficiently evaluated by the ABC method. Therefore, the same correction method of far band wings as used in the IMK code was included in the SPbSU code but only for calculations without Line Mixing. SPbSU calculations with LM do not use the χ - function.

It should be mentioned that in any case the term “difference” is considered to be “the SPbSU calculation result minus the IMK calculation result”.

The above comparison of the data calculated by the two codes yielded the following results:

- a) The slant path transmittance functions calculated by the two codes differ at all tangent heights with the exception of those below 17 km where the atmosphere is opaque in the examined spectral range;
- b) The slant path transmittance differences range from 0.005-0.01 to 0.02-0.03 of transmittance for tangent heights of 30-35 km (Fig. 12) and 17 and 20 km (Fig. 13), respectively.

We do not analyze the nature and concrete causes of these differences, as this would exceed the scope of the present report.

Similar calculations without taking the LM effect into account were also carried out for outgoing slant path radiation. The comparison revealed noticeable differences in this case. Two types of differences may be distinguished. They are referred to as selective and nonselective differences. The selective radiance differences are localized at some points of the spectrum and supposed to be caused by code distinctions in the upper atmosphere at small pressures. Comparison of the methods considering the LM effect is not aggravated, as the effect of band coupling exists in the wider spectral ranges. The nonselective differences are observed in more wide-band spectral intervals. They prevent direct comparison of the methods of LM accounting. The values of selective differences reach 1-2 mW/(m²•sr•cm⁻¹) and show a slight decrease with tangent height fall. The nonselective differences are maximum at the 17 km tangent height (Fig. 15) and reach a value slightly higher than 1 mW/(m²•sr•cm⁻¹) in the range of the Q-branch wing near 722 cm⁻¹. They decrease essentially both for larger and smaller tangent heights (Figs. 14, 16).

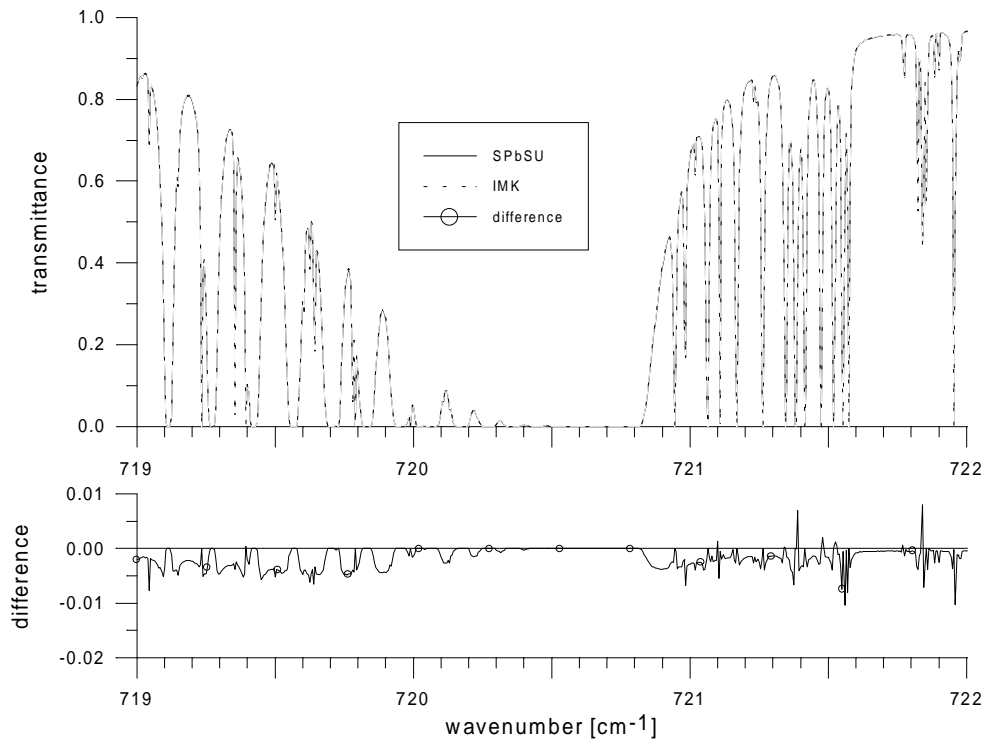


Fig. 12. Comparison of the slant path transmittances calculated by the two methods without taking into account the LM effect. Tangent height is 30 km.

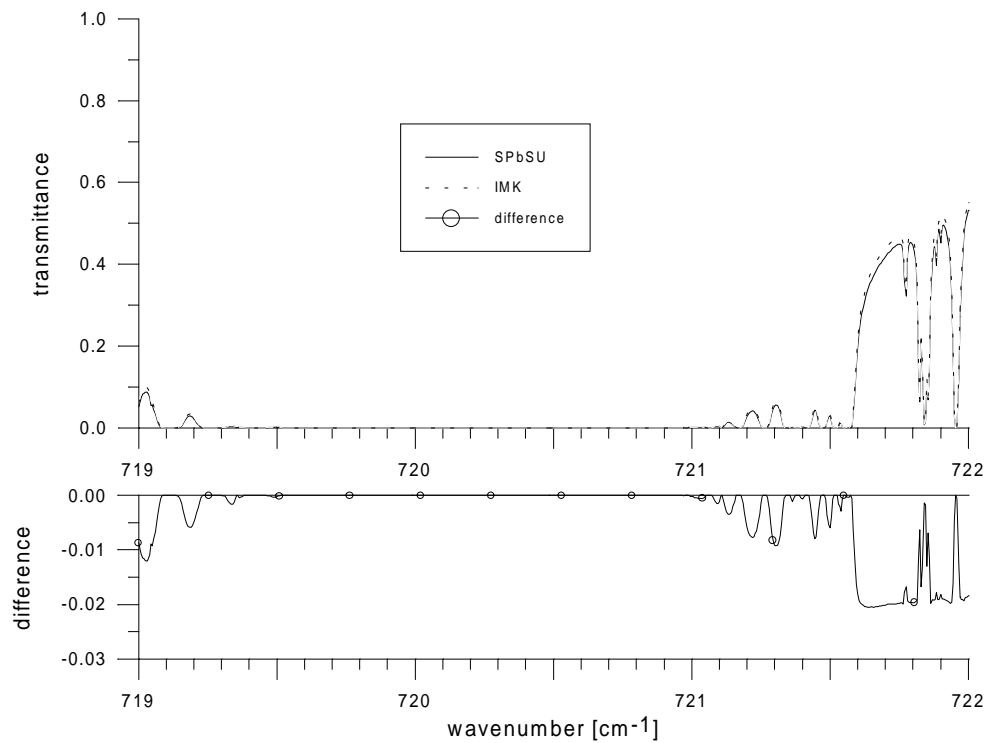


Fig. 13. Comparison of the slant path transmittances calculated by the two methods without taking into account the LM effect. Tangent height is 20 km.

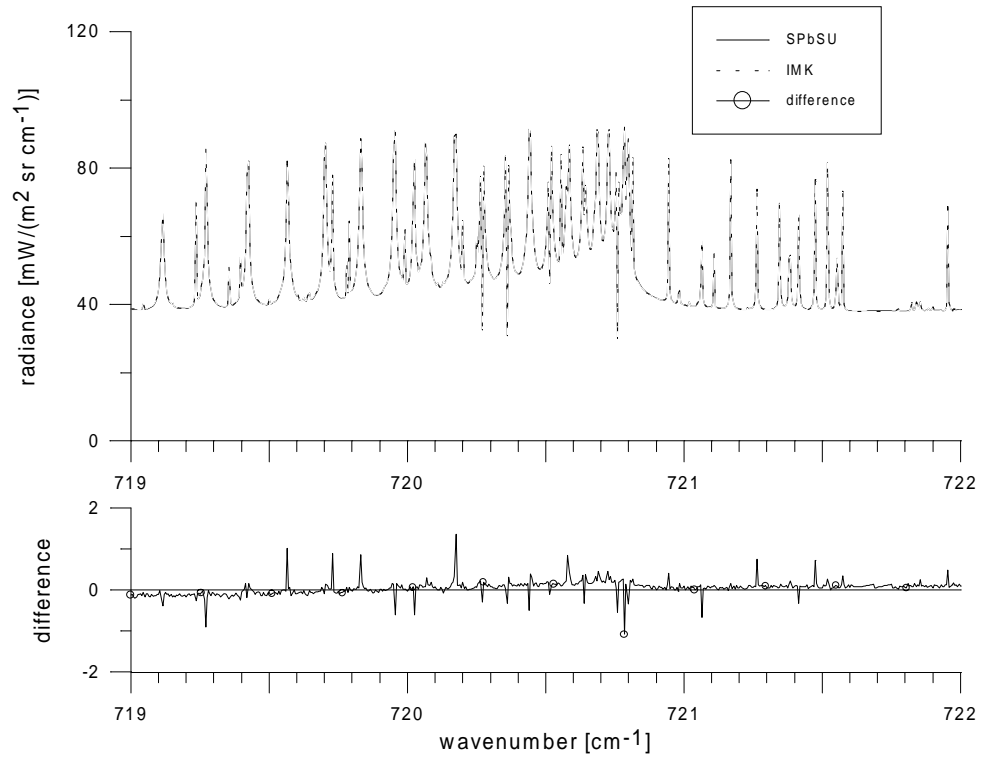


Fig. 14. Comparison of the slant path radiances calculated by the two methods without taking into account the LM effect. Tangent height is 6 km.

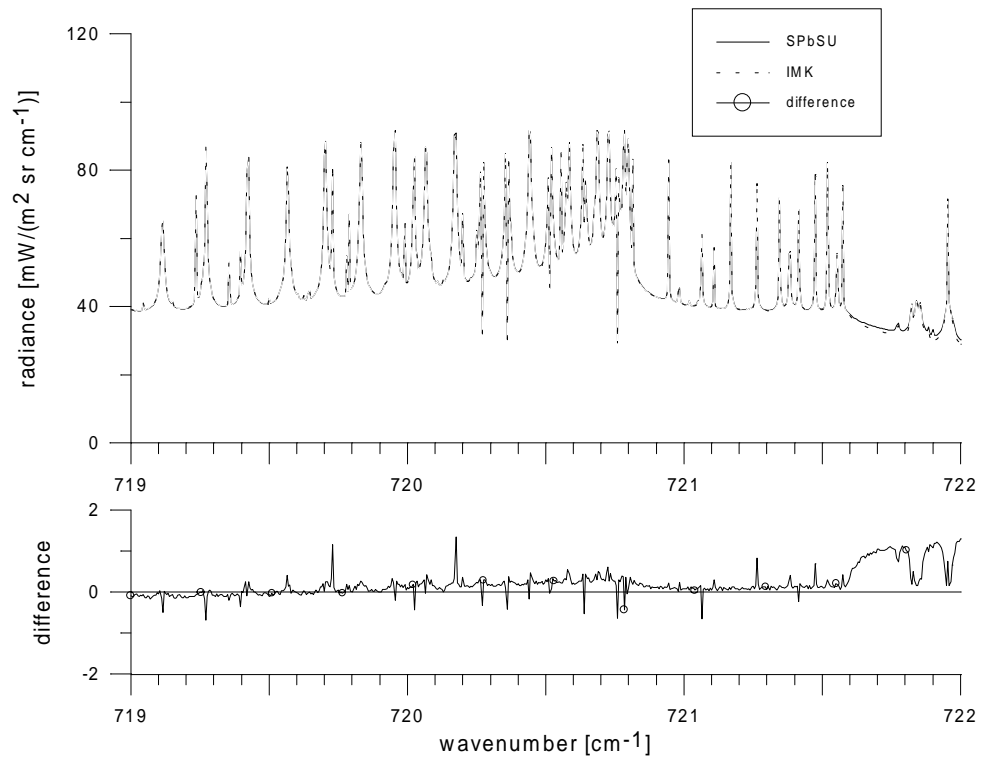


Fig. 15. Comparison of the slant path radiances calculated by the two methods without taking into account the LM effect. Tangent height is 17 km.

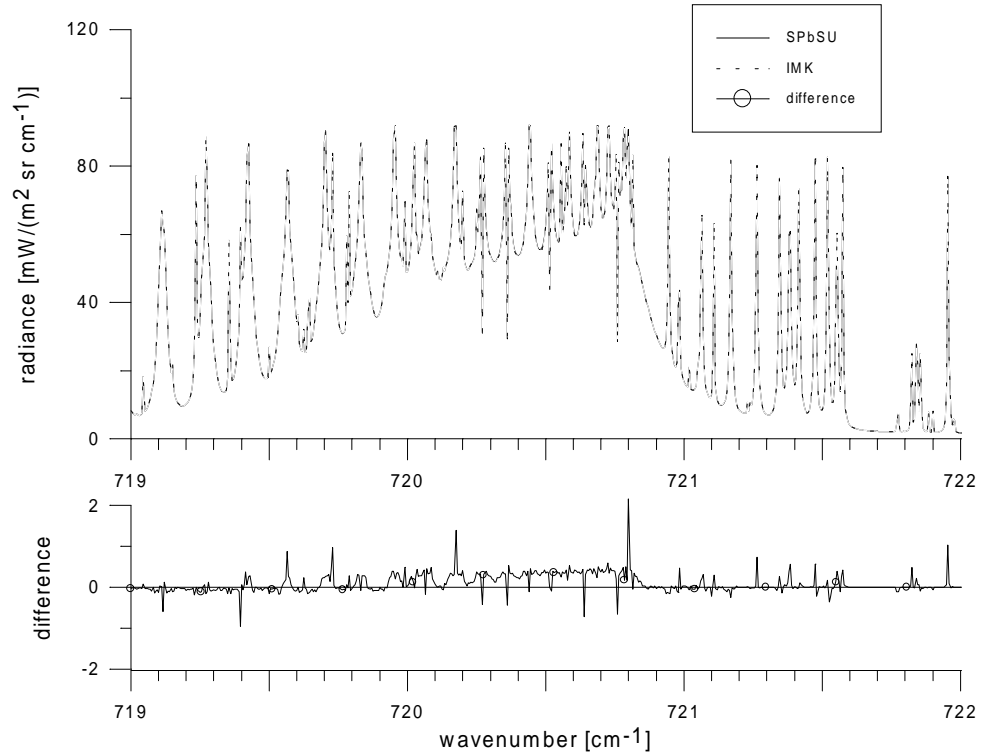


Fig. 16. Comparison of the slant path radiances calculated by the two methods without taking into account the LM effect. Tangent height is 30 km.

As shown below, the differences of the transmittances and radiances due to the different codes (without LM effect) and those due to the various methods of LM accounting are of the same order. To explain and eliminate all causes of discrepancies between the two codes, an unjustified scope of work is required. Hence, we shall compare not the transmittance or radiation calculations, but the differences between the calculations obtained by both codes with and without LM consideration.

It is evident that this approach is not fully correct, but it allows to simply compare just the methods of LM accounting and exclude other causes of differences in the calculations. During further analysis, the differences between the slant path transmittance or radiance calculations with and without LM accounting will be designated LME (Line Mixing Effect) for both computer codes.

In Fig. 17a, the slant path radiances calculated with and without LM accounting are presented for the IMK code. The lower curve in Fig. 17a represents the LME values. When correlating Figs. 15 and 17a, it is obvious that deviations between the radiance values calculated by the two codes may well exceed $1 \text{ mW}/(\text{m}^2 \cdot \text{sr} \cdot \text{cm}^{-1})$, and the LME values in the same spectral range are about $8 \text{ mW}/(\text{m}^2 \cdot \text{sr} \cdot \text{cm}^{-1})$. Such discrepancies in the calculated spectra aggravate the direct comparison of the radiances and we will match the values of the LM effect.

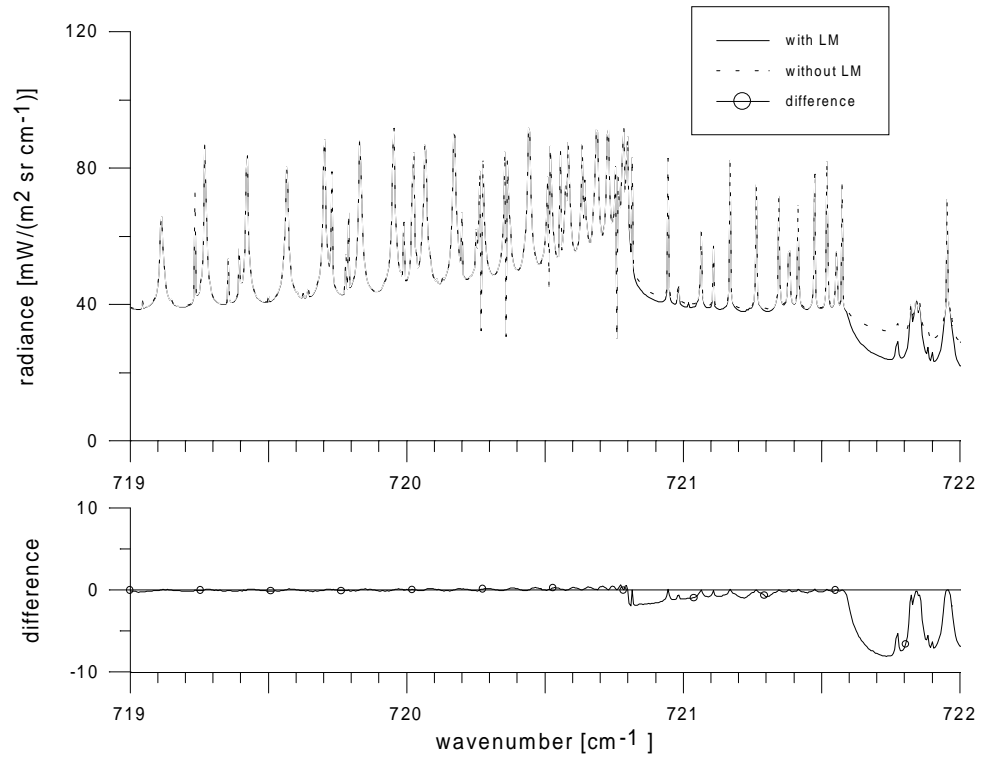


Fig. 17a. Comparison of the slant path radiances calculated with and without LM accounting by the IMK computer code. Tangent height is 17 km.

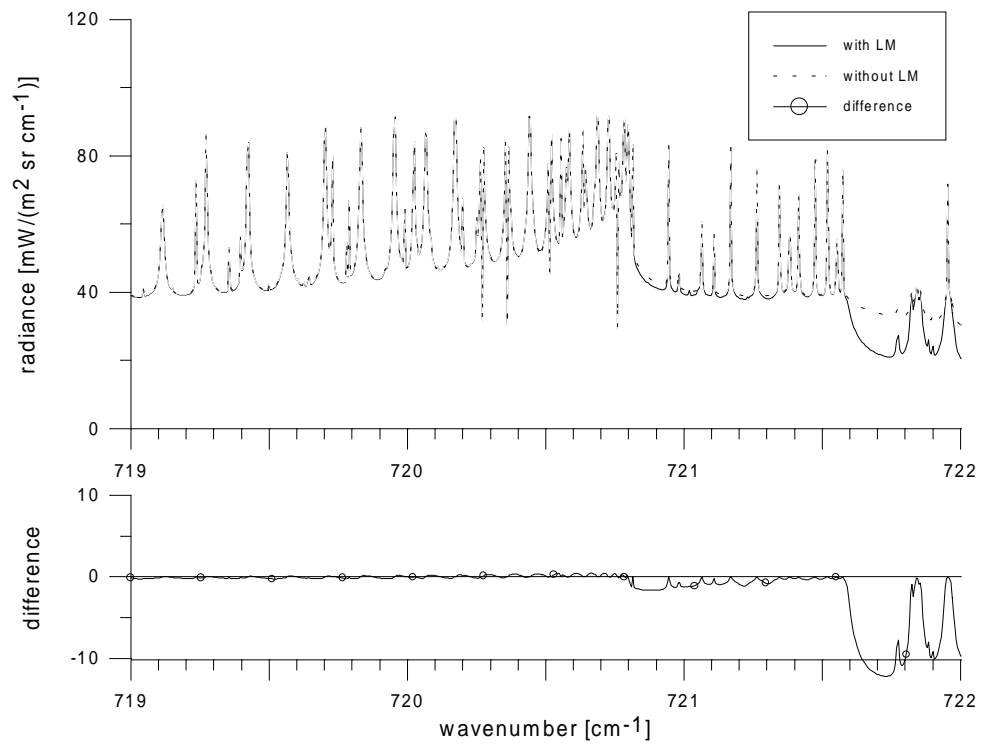


Fig. 17b. Comparison of the slant path radiances calculated with and without LM accounting by the SPbSU computer code. Tangent height is 17 km.

3.2. Comparison of the LME values calculated by the two methods

In Figs. 18-27, the LME values calculated by the two codes are represented for all examined tangent heights. Before analyzing these figures, let us consider the physical basis of the LM influence on the outgoing radiation. It must be noted that LM effects on the atmospheric transparency in the center and the wing of Q-branch are of opposite sign: absorption due to the LM effect increases in the center band and decreases in the wing. If the atmosphere is opaque in a specific spectral range at a given tangent height and the radiation originates from the higher atmospheric levels, this emitted atmospheric range is found to be higher for the Q-branch center and lower for the Q-branch wing due to the LM effect. The sign of the radiance variations is determined by the temperature profile gradient at the relevant height. In the case of atmospheric transparency, total optical thickness and radiation decrease due to the LM effect in the Q-branch wing. In the Q-branch center, the LM influence is opposite.

The situation is somewhat different for the case of the CO₂ 5-2 band. The absorption lines in the condensation range, i.e. in the Q-branch center, are characterized by a high intensity, and under Earth atmospheric conditions radiation is generated at large altitudes where the LM effect is negligible due to a small Lorenz half-width of the spectral lines. Practically all effects connected with LM become apparent in the band wings. Therefore, the LME sign is determined by the high altitude temperature gradient and atmospheric transparency in the specific spectral interval. For example, in the 720.8-721.5 cm⁻¹ spectral interval close to Q-branch at tangent heights of 6 and 8 km (Figs. 18 and 19), the absorption is large and radiation originates from the stratosphere where the temperature profile gradient is positive. Consequently, the LM effect results in a radiation decrease. In the more transparent 721.5-722 cm⁻¹ spectral interval, the troposphere with a negative temperature gradient is the main source of radiation and, as a consequence, the LME is positive. In this spectral interval at tangent heights above 11 km, the stratosphere begins to contribute to radiation. At tangent heights exceeding 17 km, this spectral interval becomes transparent. Therefore, the LME is negative at all tangent heights above 11 km. The LME values slightly depend on the tangent heights in the 720.8-721 cm⁻¹ spectral interval, where more or less the same stratospheric layer emits at all tangent heights.

Analysis of Figs. 18-27 for the purpose of comparing the two LM methods allows, first of all, to see that the results are in qualitative agreement at all tangent heights. In any case, the sign of LME, i.e. the sign of radiation difference due to LM, is the same for both methods and the LME spectral behaviors are similar. Nevertheless, essential quantitative differences occur. The LME value calculated by the SPbSU method exceeds that calculated by the IMK method (by a factor of 2) in the spectral range close to 722 cm⁻¹, i.e. in the Q-branch far band wings, at a tangent height of 8 km (Fig. 19). The LME value is about 2 mW/(m²•sr•cm⁻¹) and LME difference due to the use of the different methods is about 1 mW/(m²•sr•cm⁻¹). With an altitude increase, the relative LME differences decrease, but the absolute values of LME differences grow and reach a maximum of about 4 mW/(m²•sr•cm⁻¹) at a tangent height of 17 km (Fig. 22). Further tangent height increase results in a decrease of the LME difference.

It is interesting to note that in the spectral range adjacent to the Q-branch center near 720.8 cm⁻¹ the LME value calculated by the IMK method exceeds that of the SPbSU method for all tangent heights. However, in the remaining spectral range the sign of LME differences due to the use of the above methods is opposite. (LME denotes the difference between the radiation calculated taking into account the LM and the radiation calculated neglecting the LM, see Fig. 17a.) In other words, the SPbSU method gives a larger band narrowing far from Q-branch and a smaller band narrowing near the Q-branch as compared to the IMK method.

This was investigated in more detail by IMK. Q-branch line-mixing calculations are always performed without applying a χ - factor to Q lines within 10 cm⁻¹ of the Q-branch center, in order not to interfere with a proper line-mixing modeling. Therefore, the differences mentioned above can at the most be due to the χ -

factor usage for P- and R- branch lines within the spectral region of the Q-branch studied here. A comparison of spectra calculated by the IMK code taking into account Q-branch line-mixing and applying or not applying the χ - factor to P- and R- branch lines, respectively, is shown in Fig. 28. The tangent height the spectra are calculated for is 17 km, as at this height the maximum difference occurred. The maximum difference was found to be $5 \text{ mW}/(\text{m}^2 \cdot \text{sr} \cdot \text{cm}^{-1})$ which is about 120% of the difference between IMK and SPbSU code (see Fig 22) and has different spectral behavior. The impact of χ - factor usage at other tangent heights is much smaller and vanishes above 35 km. From this comparison we learn that χ - factor usage in the IMK code cannot explain the difference between the IMK and the SPbSU code.

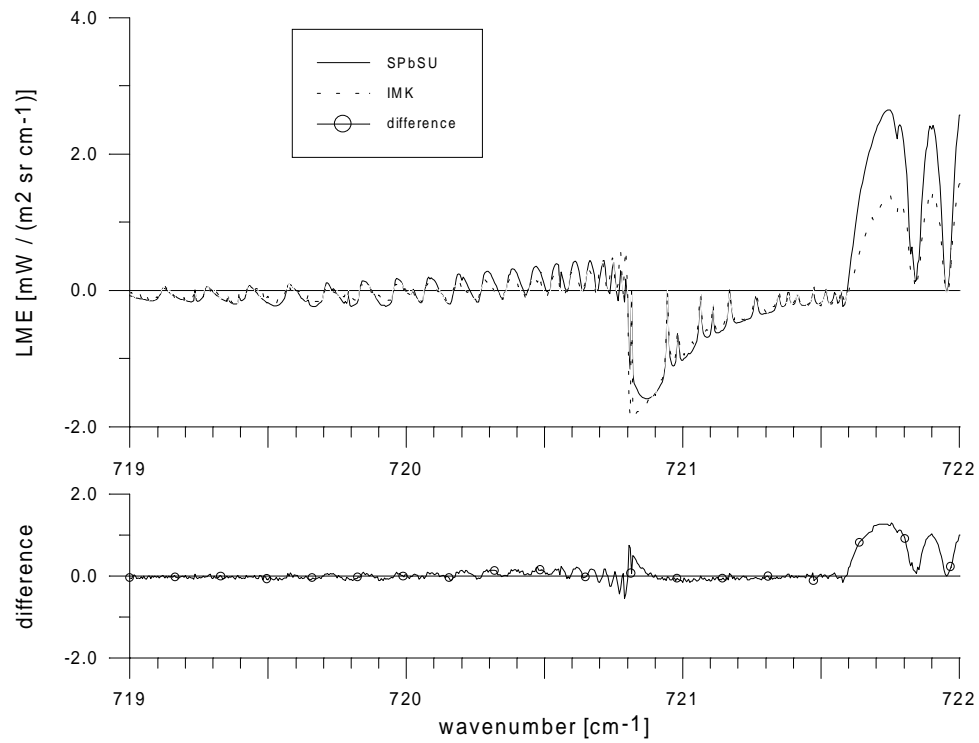


Fig. 18. Comparison of Line Mixing Effects calculated by the two methods. Tangent height is 6 km.

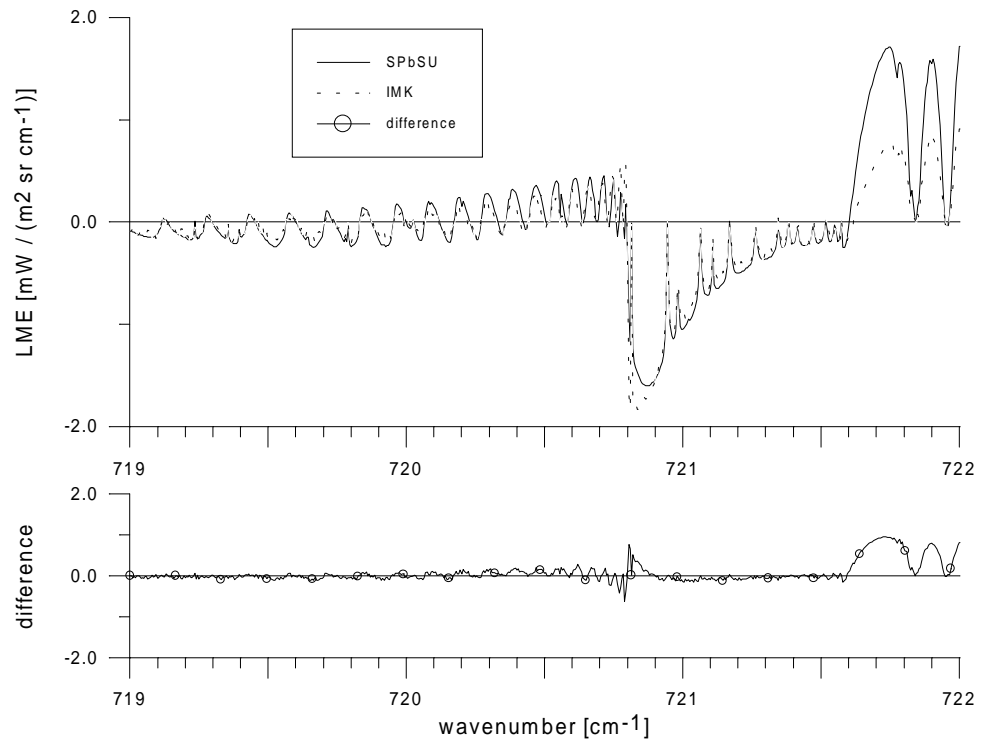


Fig. 19. Comparison of Line Mixing Effects calculated by the two methods. Tangent height is 8 km.

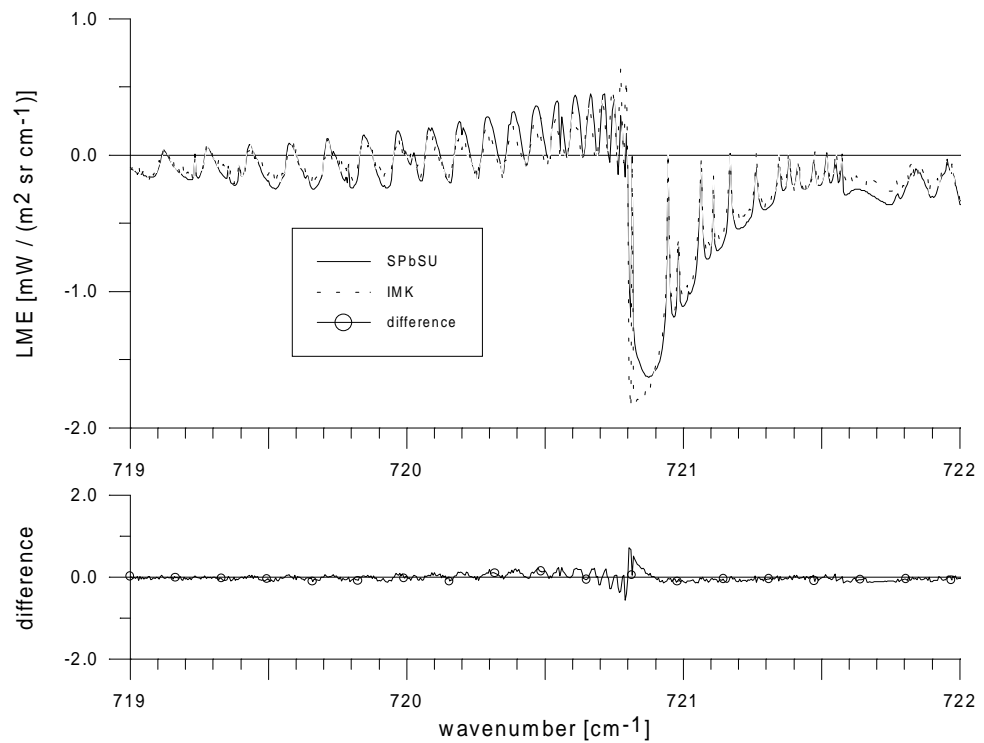


Fig. 20. Comparison of Line Mixing Effects calculated by the two methods. Tangent height is 11 km.

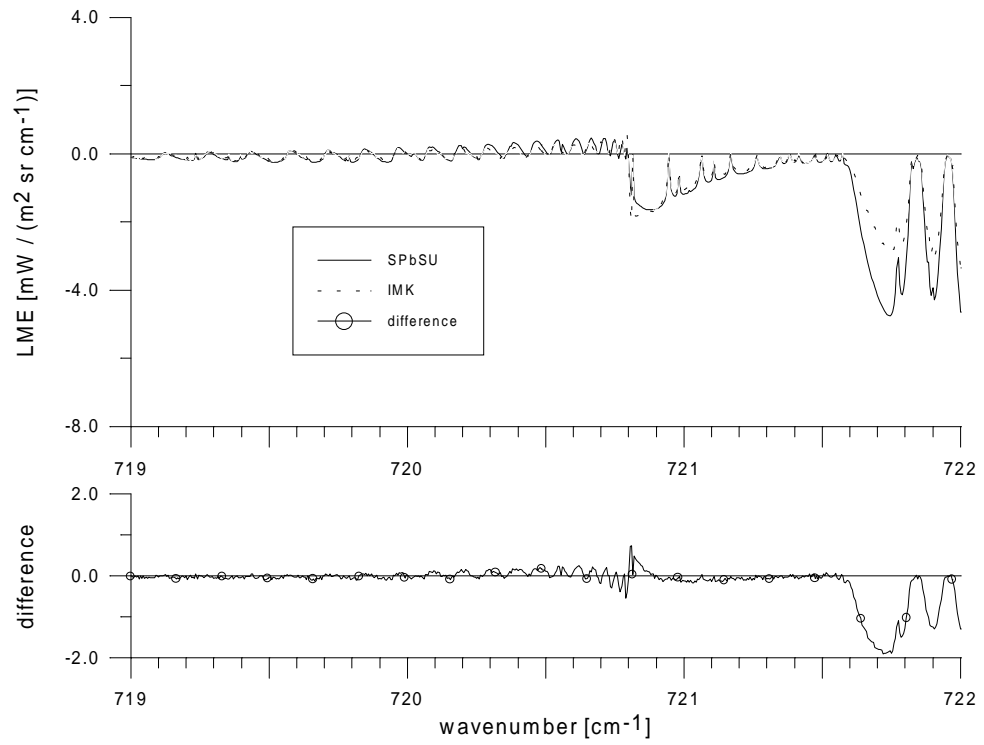


Fig. 21. Comparison of Line Mixing Effects calculated by the two methods. Tangent height is 14 km.

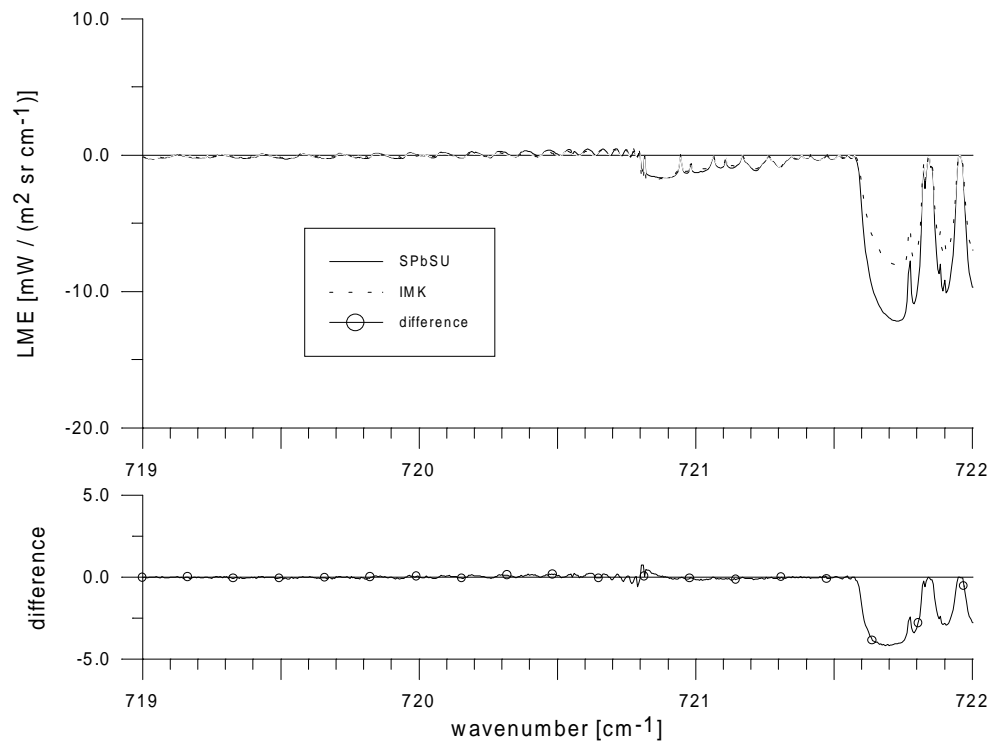


Fig. 22. Comparison of Line Mixing Effects calculated by the two methods. Tangent height is 17 km.

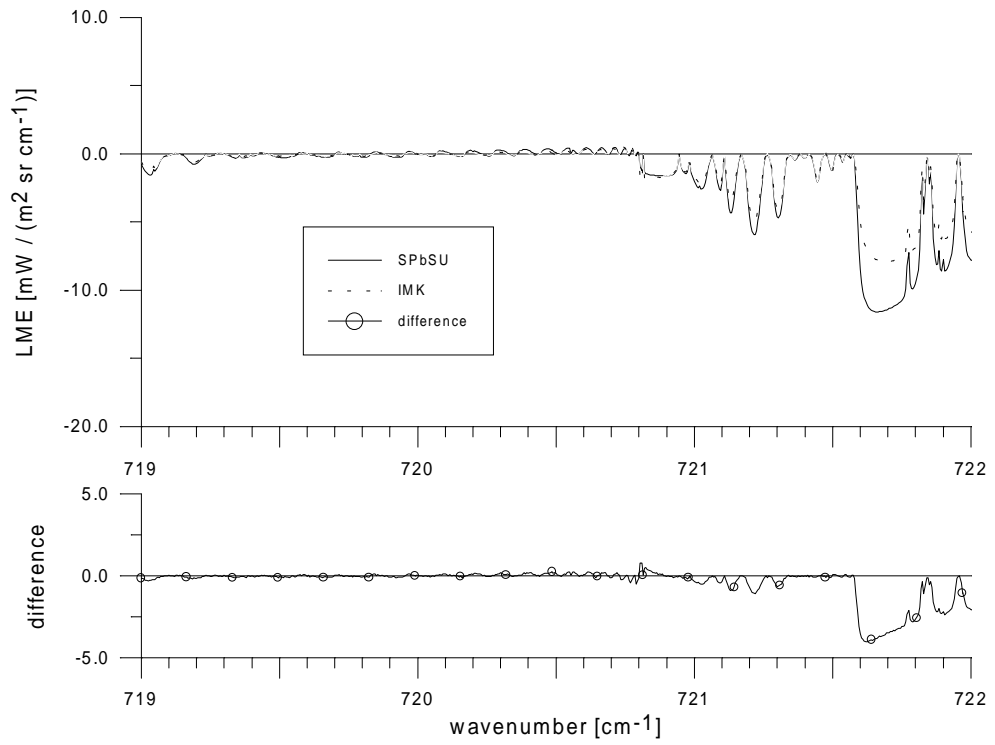


Fig. 23. Comparison of Line Mixing Effects calculated by the two methods. Tangent height is 20 km.

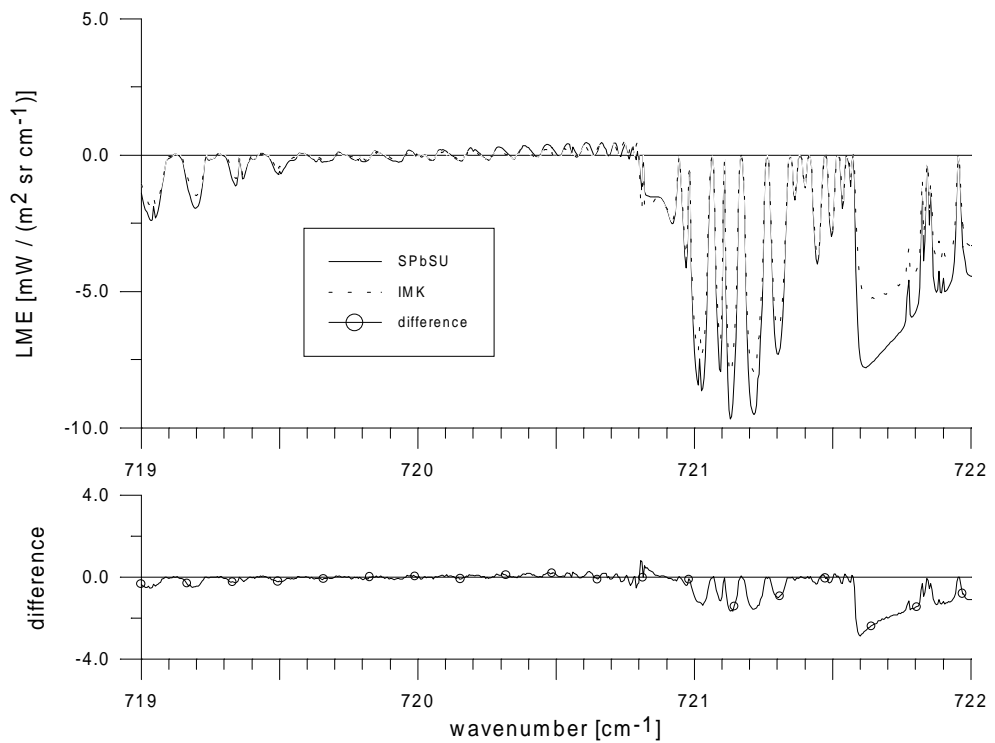


Fig. 24. Comparison of Line Mixing Effects calculated by the two methods. Tangent height is 23 km.

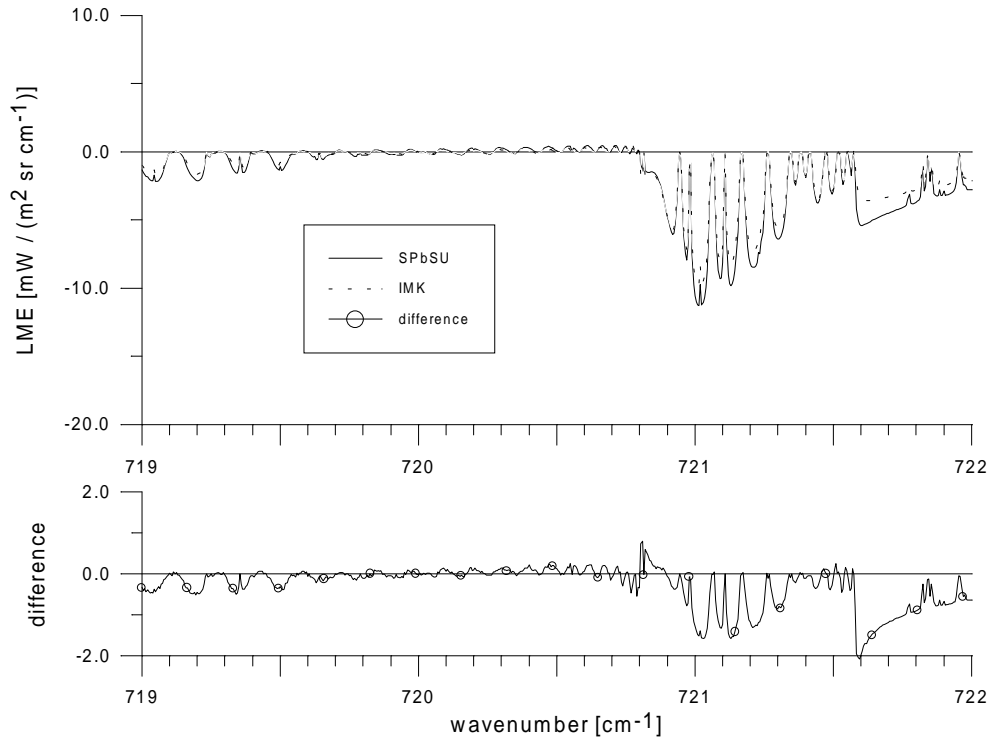


Fig. 25. Comparison of Line Mixing Effects calculated by the two methods. Tangent height is 25 km.

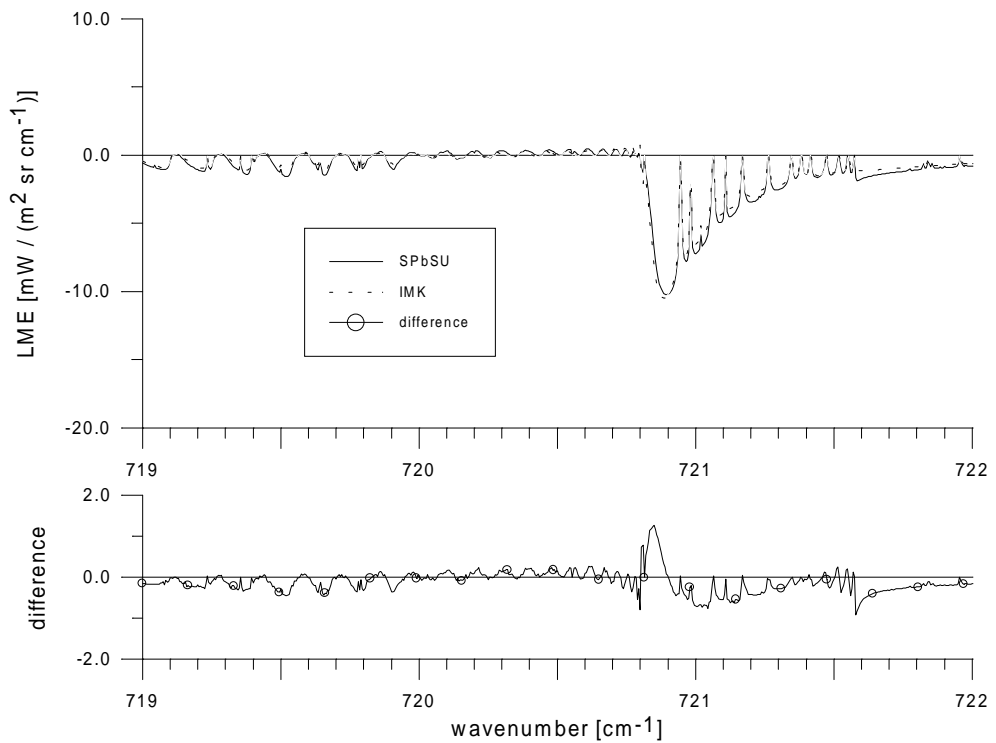


Fig. 26. Comparison of Line Mixing Effects calculated by the two methods. Tangent height is 30 km.

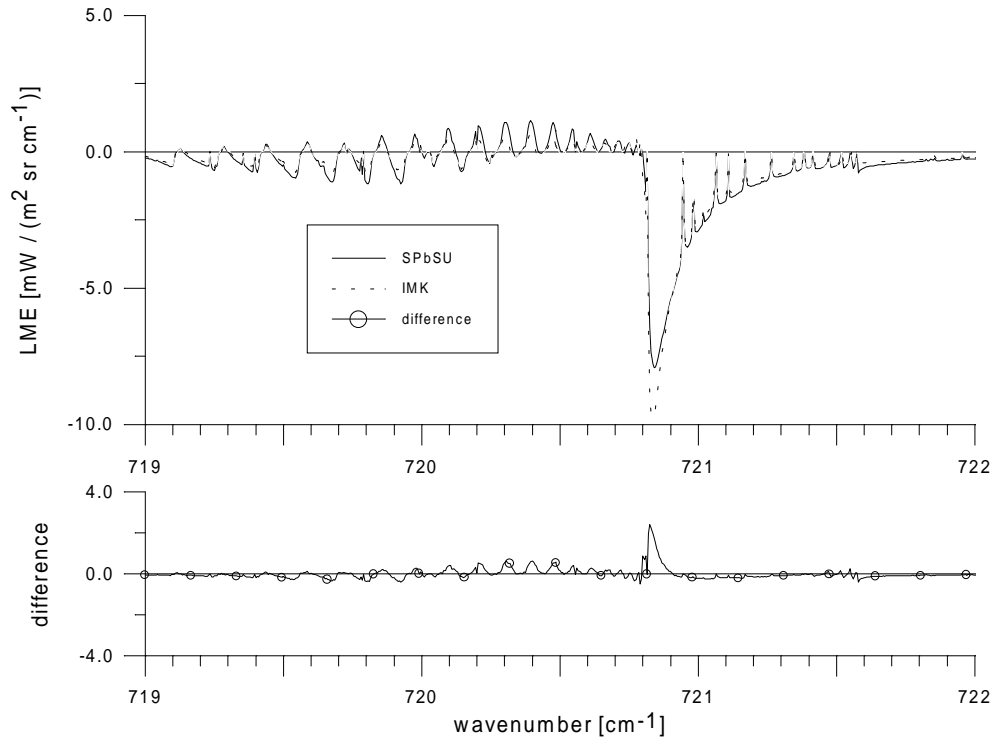


Fig. 27. Comparison of Line Mixing Effects calculated by the two methods. Tangent height is 35 km.

Furthermore, the differences between the spectra calculated without the LM and χ - factor and those calculated with the LM and χ - factor for P- and R-branch lines were investigated. The result is shown in Fig. 29. The difference spectrum is closer to the one calculated by the SPbSU code (see Fig. 17b) than the difference spectrum shown in Fig. 17a. In particular, the difference spectrum reaches values of up to 10 $\text{mW}/(\text{m}^2 \cdot \text{sr} \cdot \text{cm}^{-1})$ which is close to the maximum value of 12 $\text{mW}/(\text{m}^2 \cdot \text{sr} \cdot \text{cm}^{-1})$ of the SPbSU difference spectrum. This shows that the combined far wings and line mixing effect is equivalently taken into account by both the ABC method and the combination of Q-branch line mixing and PR-branch χ - factor modeling as applied in the IMK code.

Finally, an attempt was made to identify the partitioning of PR-branch line-mixing and far wing effects in the effect jointly modeled by the χ - factor. For this purpose, we compared a spectrum at 17 km tangent height calculated by applying pure PQR-line mixing (Bernd Funke, private communication, 1997) and a spectrum calculated by applying Q-branch line mixing and PR-branch χ - factors. The result is shown in Fig 30. It becomes evident from comparison of Figs. 30 and 28, that about 20% of the effect modeled by the usage of PR-branch χ - factors shown in Fig. 28 have to be assigned to PQR-line-mixing as modelled here, whereas about 80% of this effect must be assigned to other effects jointly modeled by the χ - factor, for example the far wing effects of the P- and R-branch lines in the region of the Q-branch, which are due to the finite duration of the molecular collisions.

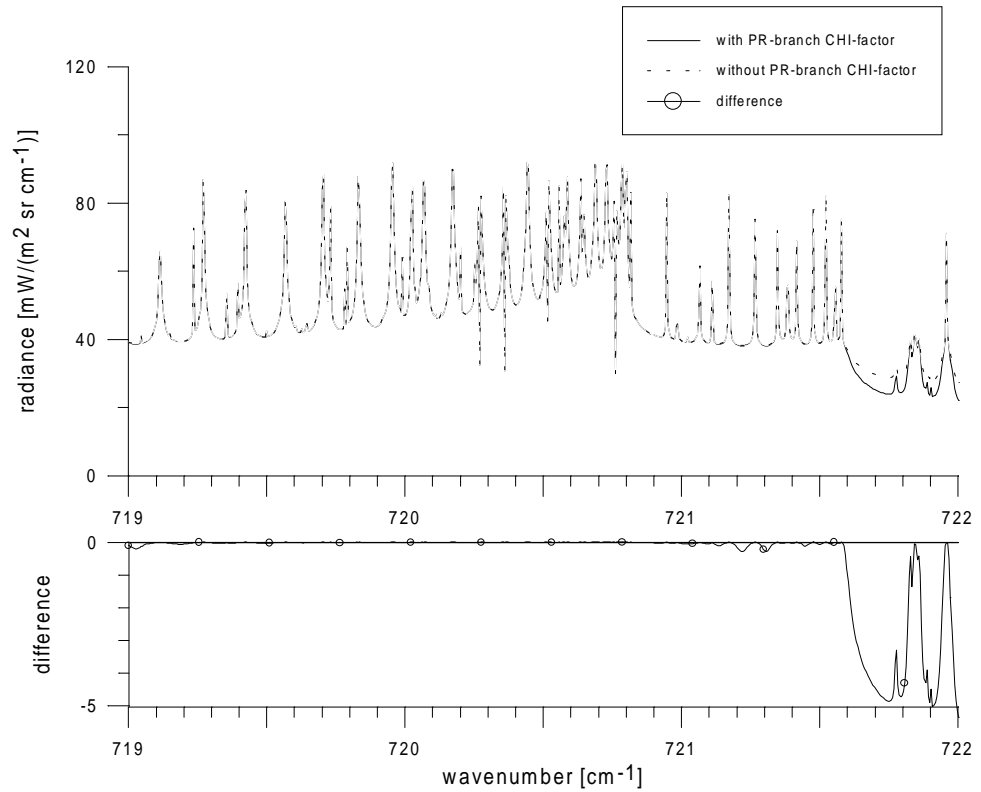


Fig. 28. Comparison of the spectra calculated with and without applying the the χ - factor to the P- and R-branch lines by the IMK code. The Q-branch LM is taken into account, tangent height is 17 km.

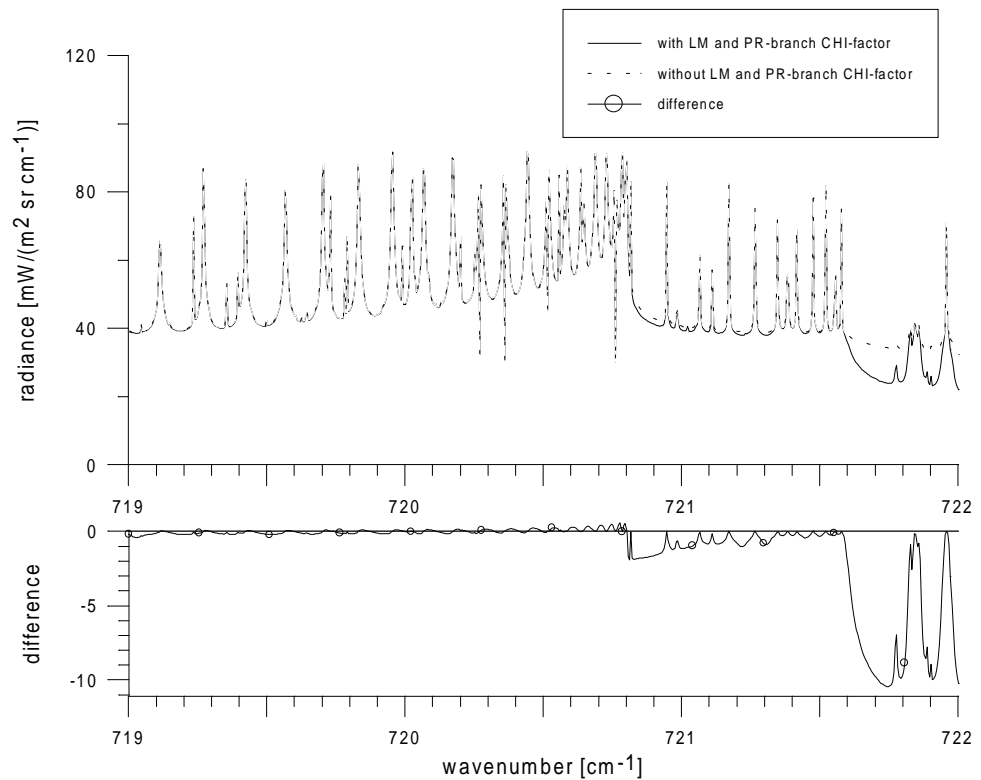


Fig. 29. Comparison of spectra calculated with Q-branch LM and applying χ - factor to P- and R- branch lines, and without both, respectively. Both spectra were calculated by the IMK code; tangent height is 17 km.

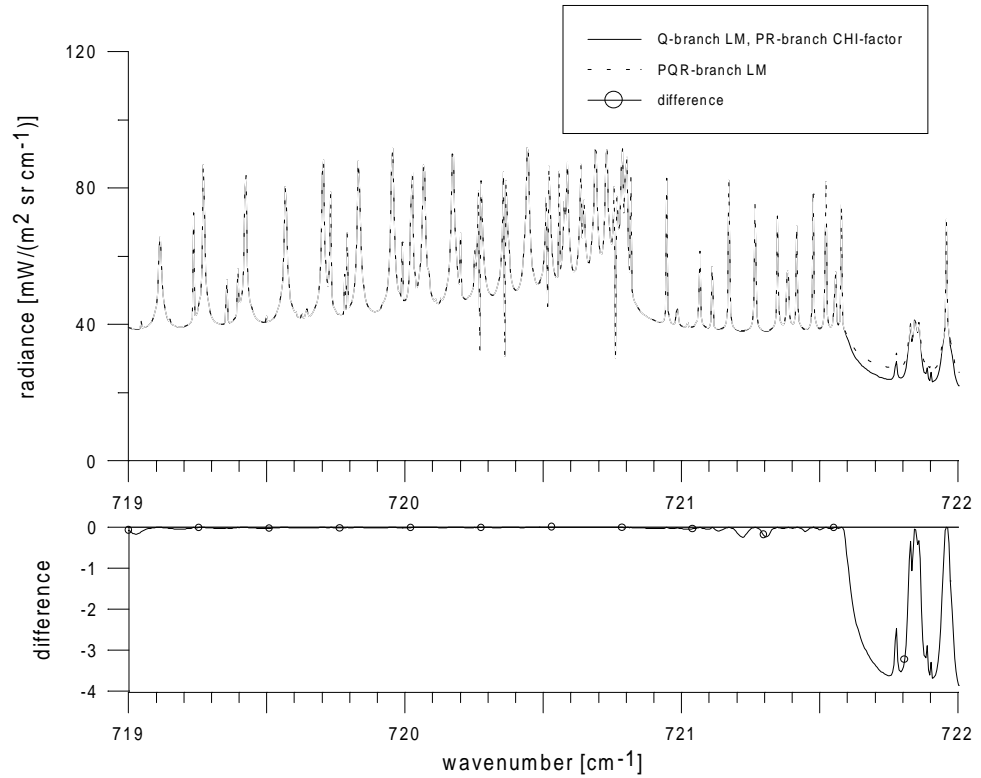


Fig. 30. Comparison of the spectra calculated with PR-branch χ - factor and Q-branch LM and with taking the PQR-branch LM into account, respectively. Tangent height is 17 km. Both spectra were calculated by the IMK code.

3.3. Summary

The calculations of atmospheric slant path radiance near 720 cm^{-1} by IMK and SPbSU codes for 6-35 km range of tangent heights revealed the following features:

- Noticeable differences between two codes prevent direct comparisons of the methods of line-mixing accounting.
- Line-mixing effect (LME) is in qualitative agreement at all tangent heights.
- The LME value calculated by the SPbSU method exceeds that calculated by the IMK method (up to a factor 2) in the spectral range close to 722 cm^{-1} , i.e. in the Q-branch band wing.
- The relative differences in the LM effect of the two methods reach about 25-30%.

4. Conclusions

Comparisons of the two methods taking into account the Line Mixing effect on the basis of experimental spectra and radiance and transmittance calculations in the spectral range near 720 cm^{-1} allow the following conclusions to be drawn:

- Both methods of LM accounting describe the LM influence on transmittance functions in qualitatively similar ways.
- Comparison of calculated and experimental spectra reveals considerable quantitative differences between the values calculated by the two codes. In the Q-branch center, differences between experimental and calculated transmittances are 0.02 and 0.06 of transmittance for the IMK and SPbSU models, respectively. The larger residual error of the SPbSU model is due to the shift of the absorption maximum inherent in the ABC method.
- The calculations of the outgoing slant path radiation exhibited a qualitative agreement of the two methods. However, the SPbSU model - ABC method - gives the larger LM effect in the wing range of the Q-branch (about $0.1 - 1.2\text{ cm}^{-1}$ away from the Q-branch center) and the smaller LM effect in the range of Q-branch center (within about 0.1 cm^{-1}) for all tangent heights as compared to the IMK method. Under strong CO_2 absorption, the values of the LM effect calculated by the two methods differ by a factor of 2 in the Q-branch wing.
- Differences of the outgoing radiation values calculated by the two methods in some cases reach about $4\text{ mW}/(\text{m}^2 \cdot \text{sr} \cdot \text{cm}^{-1})$. This value by far exceeds the MIPAS measurement error.

It must be noted that all above results were obtained by comparing the calculations with two experimental transmittance spectra for a single oscillating transition and the atmospheric radiation calculations using two methods in the narrow spectral interval only.

5. References

- Endemann M., P. Gare, D.J. Smith, K. Hoerning, B. Fladt, and R. Gessner, 1997**, MIPAS Design Overview and Current Development Status, Proceedings Europto Series, "Optics in Atmospheric Propagation, Adaptive Systems, and Lidar Techniques for Remote Sensing", A.D. Devir, A. Hohnle, and C. Werner (Eds.), European Symp. on Satellite Remote Sensing III, 24 -26 Sep. 1996, Taormina, Italy, SPIE Volume 2956, pp 124 - 135.
- Funke B., G.P. Stiller, T. von Clarmann, G. Echle, and H. Fischer, 1997**, CO_2 Line Mixing in MIPAS Limb Emission Spectra and its Influence on Retrieval of Atmospheric Parameters, *JQSRT*, **58**,1997, in press
- Hollweg H.D., V.S. Kostsov, G. Schlüssel, P. Schlüssel, Yu.M. Timofeyev, M.V. Tonkov, A.V. Polyakov, N.N. Filippov, 1995**, Interaction at mm and Optical Frequencies. Part I: Current Problems in Radiative Transfer Simulations // Final Report ESA ESTEC Contract No. 10603/93/NL/NB. //Berichte aus dem Zentrum für Meeres- und Klimaforschung. Reihe A: Meteorologie Nr. 17/ Zentrum für Meeres- und Klimaforschung der Universität Hamburg Meteorologisches Institut. 152pp.
- Hollweg H.D., V.S. Kostsov, G. Schlüssel, P. Schlüssel, Yu.M. Timofeyev, M.V. Tonkov, A.V. Polyakov, N.N. Filippov, 1995**, Interaction at mm and Optical Frequencies. Part II: Specific Atmospheric Absorption and Emission Features: Investigation and Modelling // Final Report ESA ESTEC Contract No. 0603/93/NL/NB.//Berichte aus dem Zentrum für Meeres- und Klimaforschung. Reihe A: Meteorologie Nr. 18// Zentrum für Meeres- und Klimaforschung der Universität Hamburg Meteorologisches Institut. 258pp.

Rothman L.S., R.R. Gamache, R.H. Tipping, C.P. Rinsland, M.A.H. Smith, D. Chris Benner, V. Malathy Devi, J.-M. Flaud, C. Camy-Peyret, A. Perrin, A. Goldman, S.T. Massie, L.R. Brown, and R.A. Toth, 1992, The HITRAN molecular data base: edition of 1991 and 1992, *JQSRT*, **48**, 469 pp.

Strow L.L., D.C. Tobin, and S.E. Hannon, A Compilation of First-Order Line-Mixing Coefficients for CO₂ Q-Branches, *JQSRT*, **52**, 281

Tonkov M.V., N.N. Filippov, Yu.M. Timofeyev, and A.V. Polyakov, 1996, A simple model of line mixing effect for atmospheric applications: Theoretical background and comparison with experimental profiles. *JQSRT*, **56**, No. 5, pp. 783-795.

Valentin A. and Rachet F., 1995, private communication.